


Tectonic Topography on Scandinavia's glaciated passive margin

Molde – Langfjorden – Trondheim



Photo: P. T. Osmundsen

NGU Report 2011.033
TopoScandiaDeep Field Trip
Tectonic Topography
of Norway's MTFC

Report no.: 2011.033		ISSN 0800-3416		Grading: Open	
Title: TopoScandiaDeep Field Trip, Tectonic Topography of Norway's MTFC					
Authors: T.F. Redfield, P.T. Osmundsen, S. Gradmann, M. Stokke Bauck, J. Ebbing, and A. Nasuti			Client: NGU, ESF		
County: Møre og Romsdal			Commune:		
Map-sheet name (M=1:250.000) Ålesund			Map-sheet no. and -name (M=1:50.000)		
Deposit name and grid-reference:			Number of pages: 47		Price (NOK): 210,-
Map enclosures:					
Fieldwork carried out: 2011	Date of report: 27.05.2011	Project no.: 327700	Person responsible: 		
<p>Summary: This report describes a one-day field trip to observe relationships between brittle normal faults and landscape evolution on a post-glacial passive margin. The hypothesis that the great escarpment of western Norway was shaped after the main rift phases, through reactivation of inherited faults inboard of sharply tapering crystalline crust was based on combinations of apatite fission-track dating, structural geology, topographic analysis and interpretation of offshore deep seismic and potential field data. Comprised by nine stops, the trip begins in Molde and ends in Trondheim. The total driving time is a little over five hours.</p> <p>An important theme to the field trip is the relationship between brittle faulting and large-volume rock avalanches. Many unstable rock slopes and large-volume rockslides in Norway are related to brittle faults. This is particularly true within the Møre-Trøndelag Fault Complex (MTFC), where the field trip is sited. Reactivated faults not only shaped and maintain Norway's topographically asymmetric 'Great Escarpment' - in many cases they also facilitate the landscape's efforts to return to the equipotential. The importance of post-thinning brittle faulting has been under-recognized in the onshore parts of Norway's extended margin, and it may be under-recognized also on other extended margins worldwide.</p> <p>A third theme is the change-in-paradigm that is sweeping extended margin studies. The process of hyper-extension may be more common than has previously been thought. The newly-documented connection between rift-related crustal taper, created through rifting and (hyper-)extension and subsequent landscape evolution (see Osmundsen and Redfield, in press) provides a new way to study how the emergent portions of extended margins evolve through time. Implications exist for a number of source-to sink relationships on passive margins including the evolution of landscapes, drainage and sediment routing patterns. These constitute important economic issues on more than one continent.</p> <p>This field guide provides documentation for some (although not all!) of the above. The trip begins in Molde, near the base of the Great Escarpment. The stops are situated along the damage zone of the Tjellefonna Fault, a collection of faults that comprise the innermost structures of the MTFC and that are well-exposed in roadcuts. The return to Trondheim parallels the displacement gradient suggested for the MTFC and follows the degraded great escarpment in its footwall gradient, documenting the landscape transition from faulted, deep alpine incision to unfaulted 'paleic' preservation. By day's end a panoply of sights will have documented the link between post-AFT 'closure' brittle faults, offshore architecture, and landscape evolution.</p>					
Keywords: Faults		Rockslides		Landscape	
Neotectonics		Continental Shelf		Uplift	

CONTENTS

1. Introduction.....	3
2. Background.....	5
3. Tectonic Topography on a Post-Glacial Passive Margin.....	7
4. Geological history of the Møre-Trøndelag Fault Complex	15
5. Field Trip Localities.....	20
Stop 1 – Molde Overlook	21
Stop 2 – Vik Fault	24
Stop 3 – Rød Fault.....	28
Stop 4 – Tjelle Disaster Monument.....	32
Stop 5 – Geophysical Characterization of a Segment of the MTFC	35
Stop 6 – Mulvik Fault.....	39
6. Summary and Outlook	42
7. Citations	44

1. INTRODUCTION

The purpose of this field trip is to present post-rift normal faulting as an important process in the construction and destruction of Norwegian topography. Limited by time, we will concentrate on a handful of exposures in the Møre-Trøndelag Fault Complex (MTFC) in the vicinity of Langfjord (Figure 1.1). Today's principal goal is to demonstrate the existence of a linked series of brittle faults at the base of the Great Escarpment, and to place these faults into a tectonic context.

The term '*Great Escarpment*' was introduced to the Scandinavian literature by K. Lidmar-Bergström to describe a landscape formed by river incision in an uplifted erosion surface (Lidmar-Bergström et al., 2000; Lidmar-Bergström, pers. comm., 2008). We interpret the great escarpment to reflect the topographic rise of a generalized, degraded footwall that has been upthrown relative to the hanging wall and severely degraded by erosion (Redfield and Osmundsen, 2009). The Great Escarpment marks the limit of inboard penetration of significant brittle faults in the Møre-Trøndelag Fault Complex (Figure 1.1).

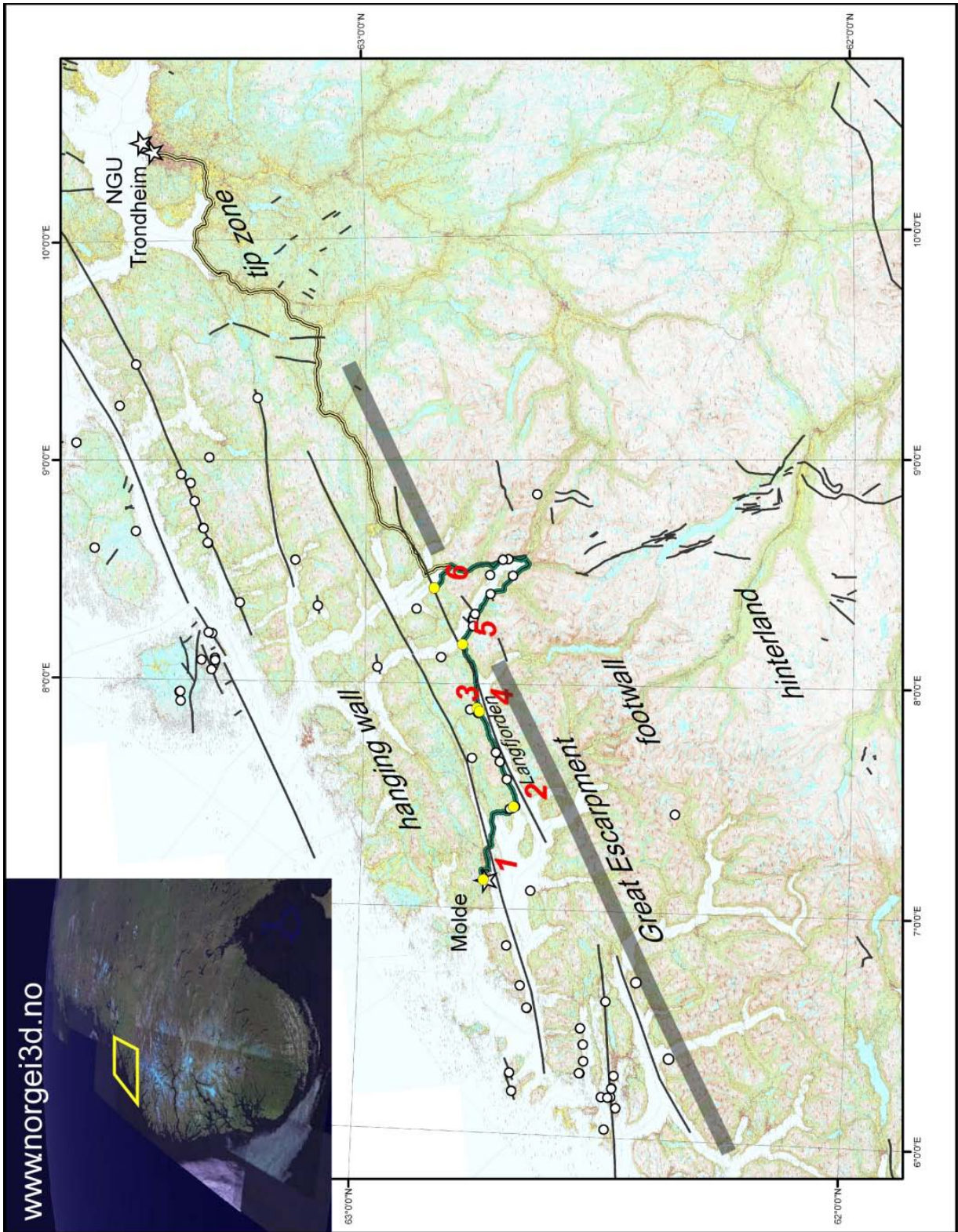


Figure 1.1: Map showing the area covered by this field trip. The route is marked by the green heavy line; our trip home is marked with the yellow superhighway symbol. Field trip stops are marked by yellow dots and red letters. In case of extra time, there are extra stop opportunities between Stop 5 and Stop 6. Black lines denote important lineaments that host fault outcrops. White circles denote individual fault outcrops. Grey band schematically depicts the Great Escarpment. Note the paucity of fault outcrops inboard of the Great Escarpment.

2. BACKGROUND

Once crustal stretching ends and extended margins enter their ‘passive’ phase, they have been generally considered to succumb to offshore thermal subsidence and onshore erosion (e.g., McKenzie, 1978). Nevertheless, many of the world’s passive margins host impressive seaward-facing escarpments (Figure 2.1; see Weissel and Karner, 1989). Despite many years of study, the mechanisms that maintain or re-establish their asymmetric topography remain controversial. Many models have been published, invoking mantle diapirs, plumes or buoyant upwellings (e.g., Rohrman et al., 1995) edge-driven convection (e.g., Faccenna et al., 2008), glacial pumping (Blundell and Waltham, 2009), lower crustal flow (Chalmers, 2011), mantle serpentinization (Olesen et al., 2006; Skelton and Jakobsson, 2007), residual Caledonian topography (Nielsen et al., 2009), far-field forces such as ridge push (Løseth, 2005), marginal uplift caused by the Paleogene opening of the North Atlantic (Torske, 1972), and the simple transfer of mass by erosion and deposition from the emergent proximal margin to the submerged distal margin (e.g. Stüwe, 1991; Redfield et al., 2005b). To date, no agreement has been achieved. We won’t resolve the issue during this field trip, but at least we can present and discuss a small sampling of geological data that must constrain the final solution.

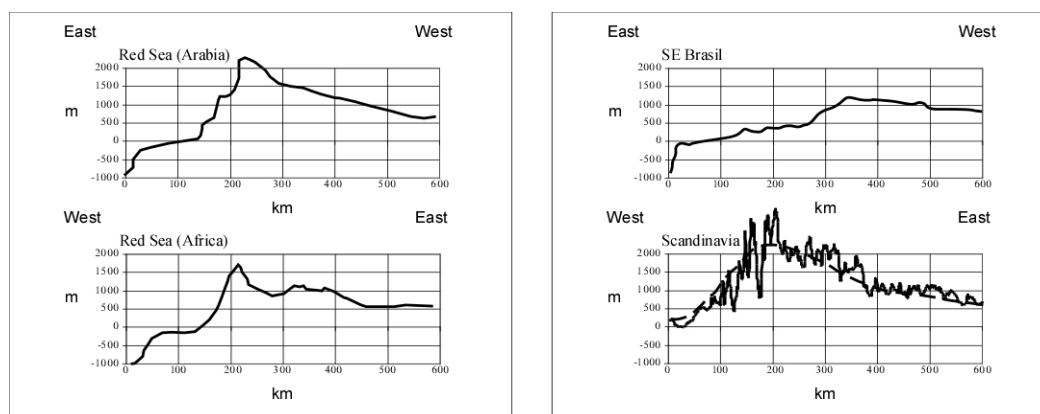


Figure 2.1: Topographic cross sections from three of the world’s passive rifted margins, taken from Weissel and Karner (1989) and Redfield et al. (2005b). In general, younger rifts evidence sharp edges (e.g., Red Sea), while older rifts are associated with eroded, gentler edges (e.g., SE Brasil). For the somewhat older margin (>55 Ma) of Scandinavia, the asymmetric shoulder of the topographic profiles (smoothed and actual) is remarkably well-defined.

On the Norwegian margin, post-breakup onshore normal faulting is a very important process. Normal fault activity clearly post-dates the main Jurassic stretching and thinning phase of the Norwegian margin, and probably post-dates earliest Tertiary breakup (Redfield et al., 2004, 2005a, b; Redfield and Osmundsen, 2009; Osmundsen et al., 2009, 2010). Understanding how these fault systems formed, and when they were active, is important for understanding the processes that formed the Scandinavian Mountains. But this isn’t all. Several catastrophic large-volume rockslide/tsunami events are documented in the Norwegian historical record. During these events, many lives were lost and much property was destroyed (e.g. Høst, 2006). Some large volume rockslides are demonstrably controlled by brittle normal faults that are part of the same fault systems.

The biggest faults tend to follow margin-parallel fjord systems, and are inaccessible except when intercepted by modern tunnelling activities. One notable exception occurs in northern Norway, near Sortlandsundet, where the hypothesis of Norwegian tectonic topography was

derived (see Osmundsen et al., 2010). Since the archipelago of Vesterålen is too far north to be part of this field trip, we refer to other publications on this topic (see Osmundsen et al., 2010; Hendriks et al., 2010; Løseth and Tveten, 1996 and citations therein). Nevertheless, the structures of Langfjorden and Sortlandsundet share many similarities. Although we cannot touch the main fault core, many smaller faults crop out in the Langfjorden structure's hanging wall. These faults provide a window on the processes of landscape formation and destruction, and form the cornerstone of our one-day excursion.

The faults we will visit are commonly characterized by zeolite minerals that formed well above the generalized brittle-ductile transition (Bauck, 2010). Many contain breccias that evince multiple events of brittle faulting (Bauck, 2010). Although reverse motion can be documented on relatively minor fault planes, kinematic indicators on the larger fault planes are dominantly normal.

Little doubt exists now within the geological community that many passive margins are not entirely passive; quite a few sectors display impressive escarpments. However, other sectors do not. Are they tectonically dead, or just biding their time? In a world of steadily-declining petroleum resources, a better understanding of the evolution of the extended margin is paramount. To that end, we state that any successful model detailing how today's Scandinavian Mountains came to be must match their observables. At a minimum, this means a successful model must:

- Generate the topographic asymmetry that is evident from the southernmost to the northernmost points of Scandinavia (Figure 3.1).
- Impose foreland and hinterland drainage patterns that resemble those that develop over active normal faults (Figure 3.2; Redfield et al., 2005b).
- Generate onshore post-thinning phase normal faults, which must have uplifted their now-degraded footwalls on the order of 3 km *after* their footwall Apatite Fission Track (AFT) *apparent ages*¹ were 'set' (Figures 3.3 and 3.4; see Redfield et al., 2004, 2005a,b; Redfield and Osmundsen, 2009; Hendriks et al., 2010).
- Generate linear belts of seaward-facing alpine topography (see Osmundsen et al., 2010; Figure 3.5).
- Generate the westward fanning, eastward converging arrangement of paleosurfaces (Figure 3.6; see Lidmar-Bergström et al., 2007).
- Generate thick Tertiary offshore sedimentary deposits with their appropriate unconformities.
- Accommodate Bouguer gravity lows on the order of -150 mGal whose minima are ever-so-slightly, yet consistently, offset inboard from the actual topographic crest.

¹ The number we call an AFT age reflects several known factors such as the rate of cooling and the crystal chemistry, and probably several unknown other ones as well. (See discussion in Redfield, 2010). Hence for AFT data we use the term *apparent age*.

3. TECTONIC TOPOGRAPHY ON A POST-GLACIAL PASSIVE MARGIN

We have hypothesized that uplift and landscape formation in western Scandinavia was associated with slip along normal faults (see Redfield et al., 2005b; Osmundsen et al., 2009, 2010; Redfield and Osmundsen, 2009). Below, we will review some of the observations that lie behind our hypothesis.

- **Topographic asymmetry:** Figure 3.1 illustrates the long-wavelength topographic asymmetry of Scandinavia (see Munch, 1850; Holtedahl, 1953; Redfield et al., 2005a,b). The generalized land surface rises gently from the Gulf of Bothnia over some 300 to 400 kilometres as a largely unbroken hinterland slope, until it meets the topographic crest. Two general highland regions are linked across mid-Norway region by what appears as a mega-relay at the intersection of the NE end of the Møre-Trøndelag Fault Complex (MTFC) and lower mountain peaks (see Redfield et al, 2005b). West of the crest, elevations drop abruptly. Scandinavia's tilt-block shape and the sharpness of the escarpments in the highland regions are remarkably similar to the topography of areas undergoing active normal faulting.

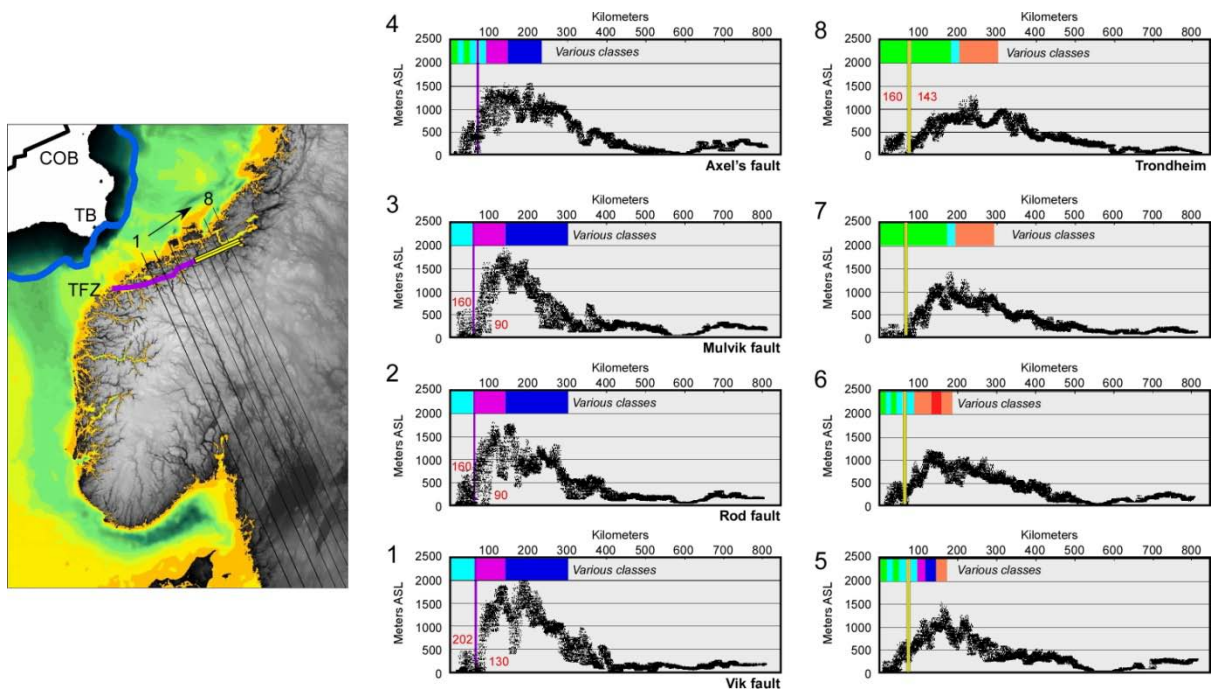


Figure 3.1: Left: map showing COB = Continent Ocean Boundary. TB = Taper Break (see also Redfield and Osmundsen, 2011, and Osmundsen and Redfield, in press). TFZ = Tjellefona Fault Zone. Profile lines are drawn perpendicular to the TFZ. Right: topographic profiles from 800m resolution DEM showing location of the Tjellefona Fault Zone relative to the stunning topographic rise we have taken to identifying as the Great Escarpment. Vik, Rod, and Mulvik faults (stops 2, 4 and 9), shown by purple vertical lines, lie exactly at its base. Red numbers indicate near-sea level AFT apparent age juxtapositions. Color bar at top indicates contrast in landscape classes of Etzelmüller et al. (2007) across the TFZ (see also Figures 3.5, 5.2.3 and 5.6.2).

- Asymmetric drainage patterns typical of normal fault landscapes, at the regional and continental scale:** Empirical and experimental evidence shows that hillside slopes constitute an extremely important function controlling the evolution of drainage patterns (see Phillips and Schumm, 1987). Models of drainage evolution in actively extending terranes (e.g., Leeder and Gawthorpe, 1987; Leeder and Jackson, 1993; Gawthorpe and Leeder, 2000) are also very well controlled by observations. Scandinavia's higher-order drainages illustrate the asymmetry and organization typical of active footwalls and their hinterland backslopes (Figure 3.2). At the MTFC's more regional scale, the curved form of an inboard drainage mimics the diversion typical at an actively-propagating normal fault tip (Figure 3.2; see also Figure 4.2). Lastly, several instances of drainage capture (the 'agnor' valleys) are well-documented (Figure 3.2). Whilst the captures may reflect a variety of causes, they are consistent with tilt-block style tectonic uplift.

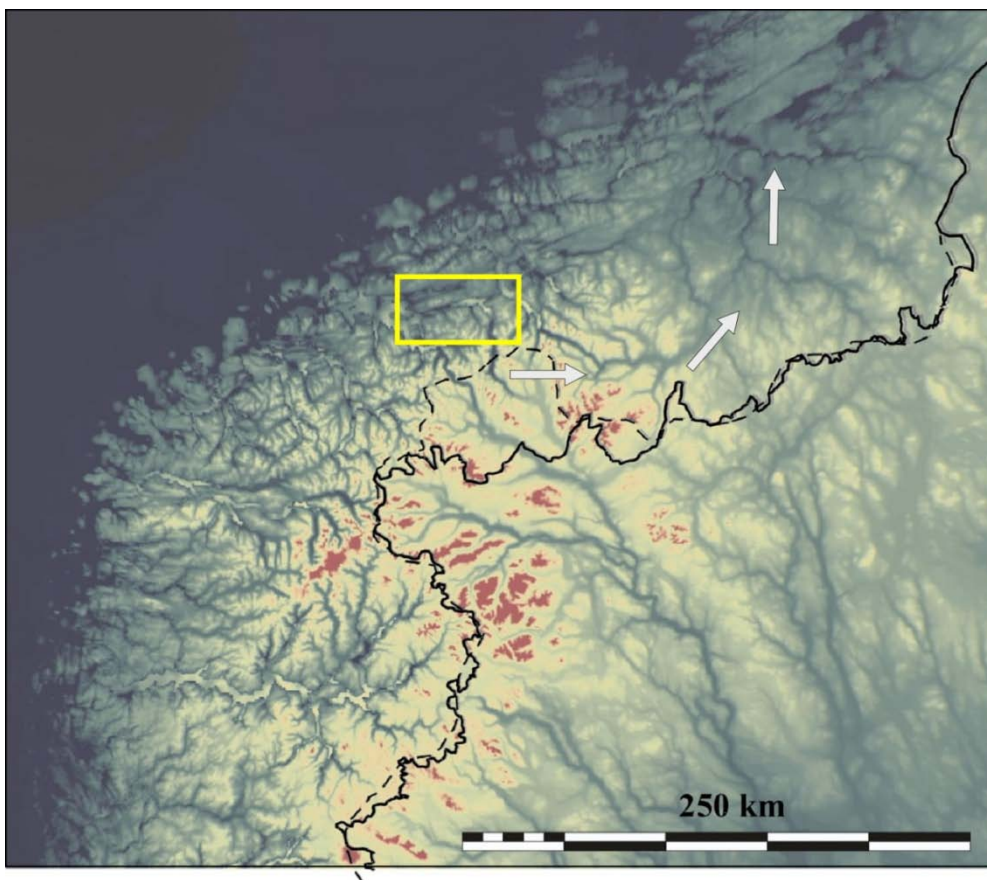


Figure 3.2: GTOPO5 Digital Elevation Model shaded to emphasize the drainage patterns of southern Norway. The present-day drainage-divide is shown as a solid black line. The dashed line illustrates a paleodrainage divide defined by the so-called 'agnor' valleys. The image illustrates the differences in length between drainages east and west of the divide, as it is expected for regions of different slope angles (Phillips and Schumm, 1987). White arrows illustrate a curved drainage system that appears to have been diverted by continued normal growth of the MTFC tip. Yellow box encompasses Langfjord.

- Short wavelength apatite fission track juxtapositions:** Figure 3.3 illustrates the short-wavelength offsets of differently-cooled structural units within the MTFC. An apatite fission track ‘age’ represents a temperature between about 60 and 110°C, depending on cooling rate; slow-cooled samples such as those of Figure 3.3 might be reasonably considered in terms of about 90 degrees. Sharp ‘jumps’ in apparent age and track length distribution occur across topographically-pronounced lineaments (Redfield et al., 2004, 2005a; Redfield and Osmundsen, 2009), many of which are now known to contain brittle fault products such as those we shall see at Stops 2, 3, and 9. Rohrman et al. (1995) interpreted the overall AFT pattern to reflect a symmetric and domal exhumation. However, Redfield et al. (2005a, b) combined Rohrman’s existing data with new data and suggested the AFT pattern more aptly depicts a series of down-to-the-northwest (normal sense) relative offsets (Figure 3.4). Redfield et al. (2005b) explicitly related the AFT age pattern in the MTFC to a normal fault displacement gradient (see Figure 4.2).

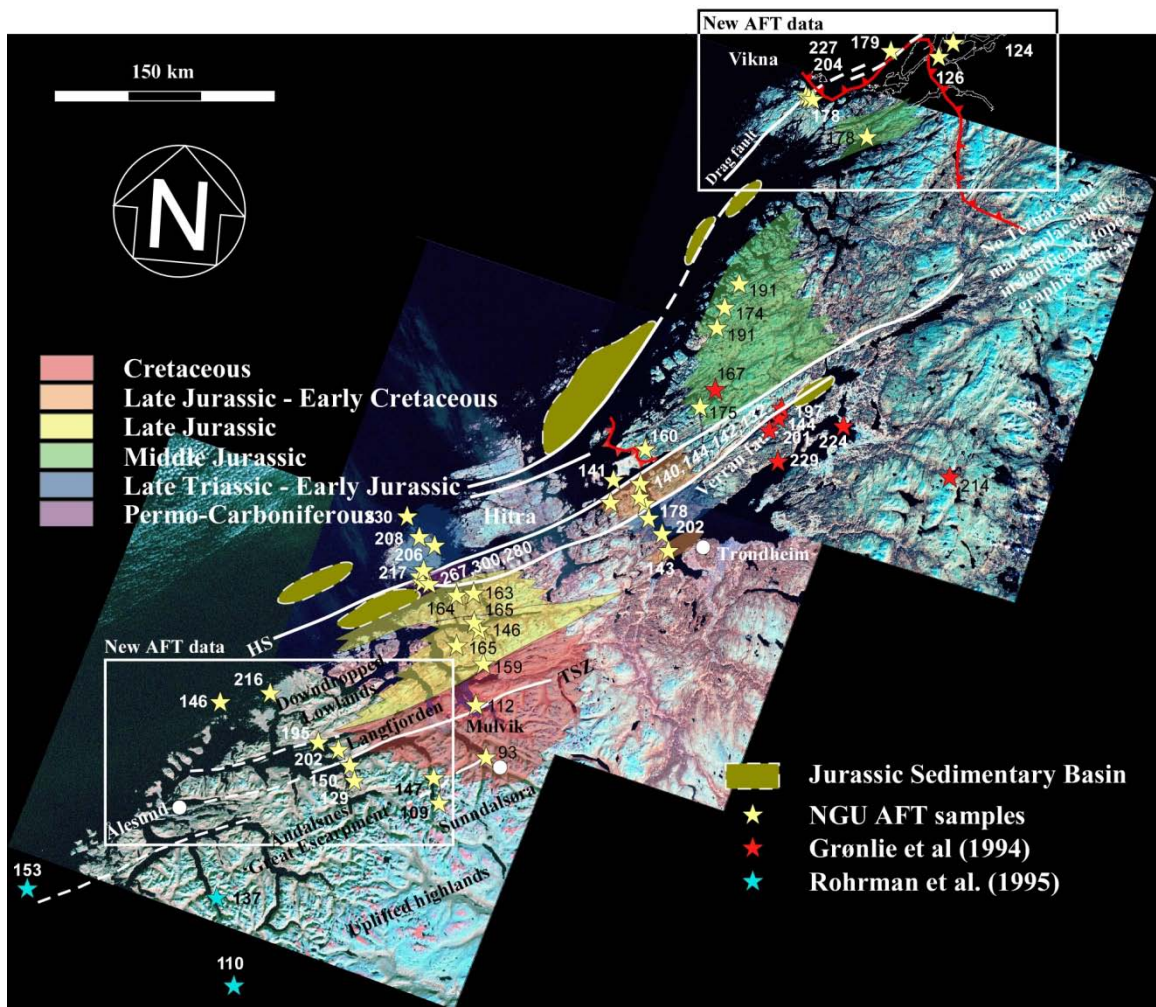


Figure 3.3: AFT sample site and apparent age map after Redfield et al. (2005b). Yellow stars denote individual sample sites reported in Redfield et al. (2004, 2005a). Additional sample ages from near Molde were reported in Redfield and Osmundsen (2009). Color coding denotes AFT apparent age zones. White lines represent lineaments within which fault rocks have been found. Detachment faults marked in red document Paleozoic extension (see Osmundsen et al., 2006; Braathen et al., 2000).

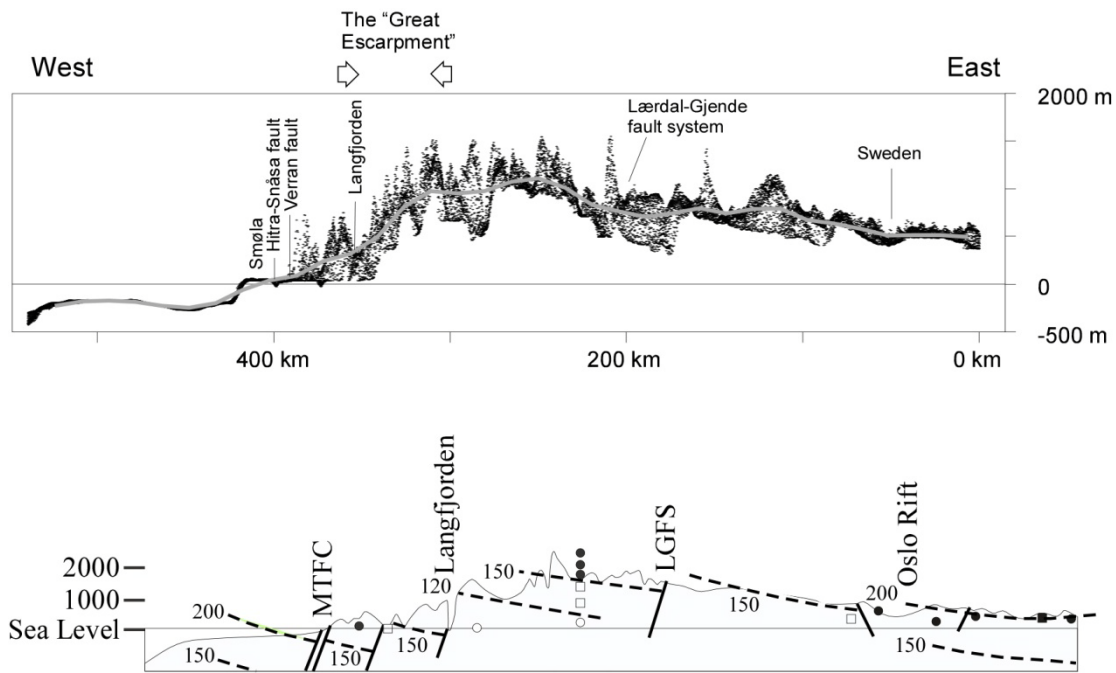


Figure 3.4: Top: topographic cross section through Norway’s Great Escarpment. This is a post-glacial passive margin, yet its long-wavelength similarity with the topographic profile of a normal fault controlled tilt block is striking. Bottom: cartoon illustrating our 2005 reinterpretation of Apatite Fission Track data of Rohrman et al. (1995). Figures modified from Redfield et al. (2005a, b).

- **Fault-bounded linear belts of alpine topography:** Figure 3.5 shows a portion of the classification of Scandinavian DEM data by Etzelmüller et al. (2007). Scandinavia’s alpine landform classes do not generally occupy her highest elevations; rather, Osmundsen et al. (2010) recognized that much of Norwegian ‘alpine’ topography occurs on the seaward-facing escarpments. In the Langfjorden region, the alpine classification displays a particularly sharp linear boundary coincident with the Tjellefonna strand of the MTFC. Osmundsen et al. (2010) suggested this observation can be best explained by a model invoking preferential erosion of dense drainage networks that evolved atop previously-uplifted normal fault footwalls (See Figure 5.1.3).

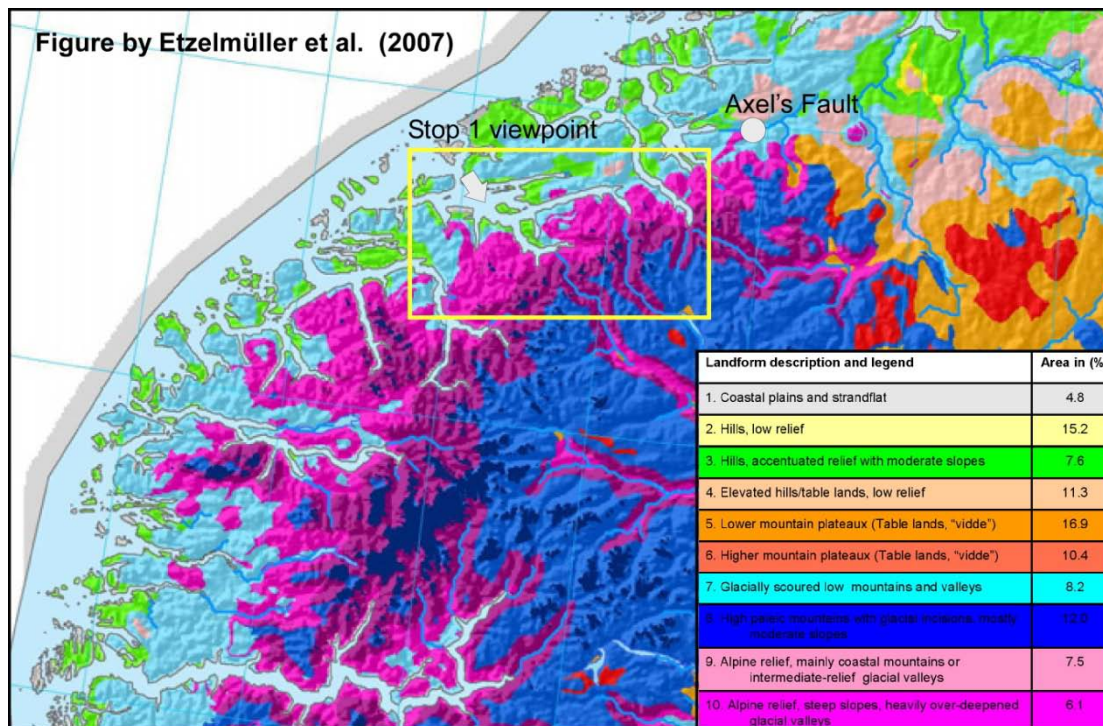


Figure 3.5: Enlarged section of Figure 7 of Etzelmüller et al. (2007) showing 10 landscape classes determined from a Digital Elevation Model. Magenta pixels represent Alpine relief (Class 10: steep slopes and heavily-oversteepened glacial valleys) whilst dark blue pixels represent high 'paleic' mountains with glacial incisions and mostly moderate slopes. Note the sharply linear nature of the boundary between the Alpine class and the coastal classes in the Langfjorden region (yellow box). The actual land surface elevations of the high paleic mountain domain in the yellow box are higher than the Alpine domain: glacial excavation occurred preferentially on the dense drainage network of the degraded footwall. The short distance involved precludes a simple difference in climate caused by 'rainshadow' between footwall and hinterland. White arrow denotes viewpoint direction of Stop 1 (Figure 5.1.2). White dot labeled Axel's Fault is the northernmost brittle fault belonging to the Tjellefonna Fault Zone that we know of to date. Note its location near the end of the linear belt of Class 10 'alpine' landforms.

- **Westward fanning, eastward converging arrangement of paleosurfaces:** Careful mapping by K. Lidmar-Bergström and her students produced Figure 3.6. In much of northern Norway a fanning arrangement between major erosion surfaces are preserved within the Northern Scandes. They are all inclined to the ESE, are 300-400 m apart within the mountains, and merge more or less east of the mountains (Lidmar-Bergström et al., 2007). The paleosurface fan matches the topographic asymmetry; a one-to-one relationship between tectonically-imposed topography, drainage, and surface preservation or destruction seems indicated.

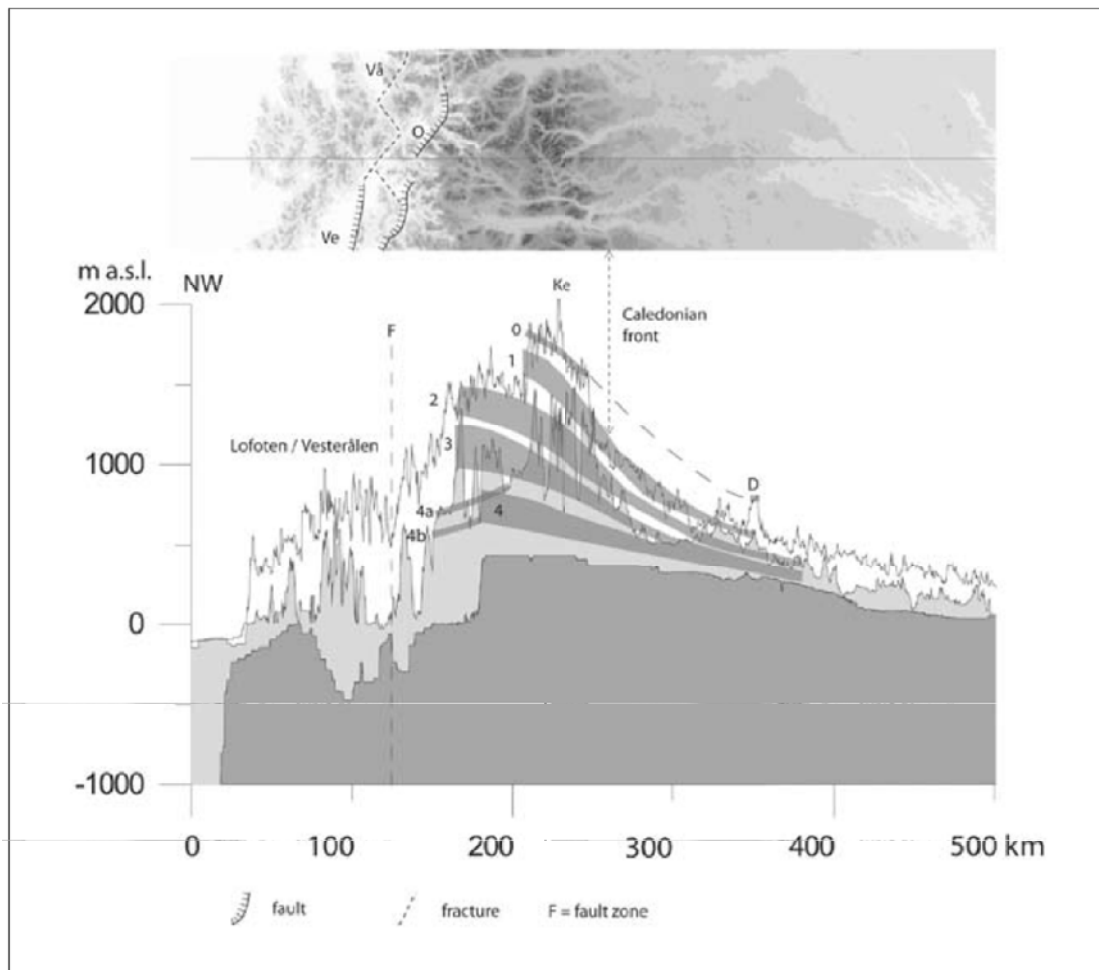


Figure 3.6: Figure from Lidmar-Bergström et al. (2007) showing a regional profile across the Northern Scandes (NS) and its eastern flank with maximum and minimum values extracted from a 130 km wide zone along the profile. Four fluvial surface/valley generations dip towards ESE all the way from the Norwegian coast. They join more or less in the east with generations 3 and 4 making up the floor of the Muddus plains. Faults in the eastern Vestfjorden, and east of Vågsfjorden and Ofotfjorden are interpreted to have guided an uplift centre close to the coast. The escarpment at the coast is 500 m high from generation 4b. The bottom profile shows the lake levels of the glacially eroded main valleys. The step in the bottom profile in the west shows the backward incision of the fjord valleys. F = fault. Ve = Vestfjorden. O = Ofotfjorden. Vå = Vågsfjorden. Ke = Kebnekajse. D = Dundret.

- ***The taper of the crystalline crust:*** We have derived an observationally-based scaling relationship determined from more than 40 of the world's extended margins including Scandinavia's (Figure 3.7; Osmundsen and Redfield, in press). The relationship links thinning-phase crustal architecture to escarpment elevation through the location of the *taper break*. The taper break is defined as the innermost point where the crystalline crust has been tectonically thinned to 10 km thickness. Conceptually, as well as in the well-imaged Norwegian example, the taper break is located close to the hanging-wall cutoff for the first fault-block in the distal margin – the outer limit of the 'necking zone'. This definition of crustal taper and taper break has its roots in the new hyper-extension models for passive margin formation (e.g., Péron-Pinvidic and Manatschal, 2009). The 'Taper Rule' states that the closer to shore is the taper break, the higher will be the seaward facing escarpment (Figure 3.7).

The Taper Rule places the ultimate origin of today's escarpments firmly on the structural architecture that, in Norway, formed during Jurassic era crustal thinning. It is a direct child of the new models of how continents break apart (e.g., Péron-Pinvidic and Manatschal, 2009), and links syn-rift to post-rift time through a direct continuum. However, the Taper Rule does *not* imply that syn-rift escarpments generated by tectonic excision must persist from the time of their inception until the present day. Indeed, in the Norwegian case it is virtually impossible: sea level AFT apparent ages from crystalline bedrock at the base of the degraded footwalls are all younger than the Jurassic. They are slow-cooled, and the several kilometers of vertical exhumation required to expose them from mid-APAZ depths must have required significant footwall uplift in post-thinning phase time. Escarpments may degrade; their topography may be reduced; *but when the time comes, they seem to be preferentially rejuvenated where the crustal taper is sharp to very sharp.*

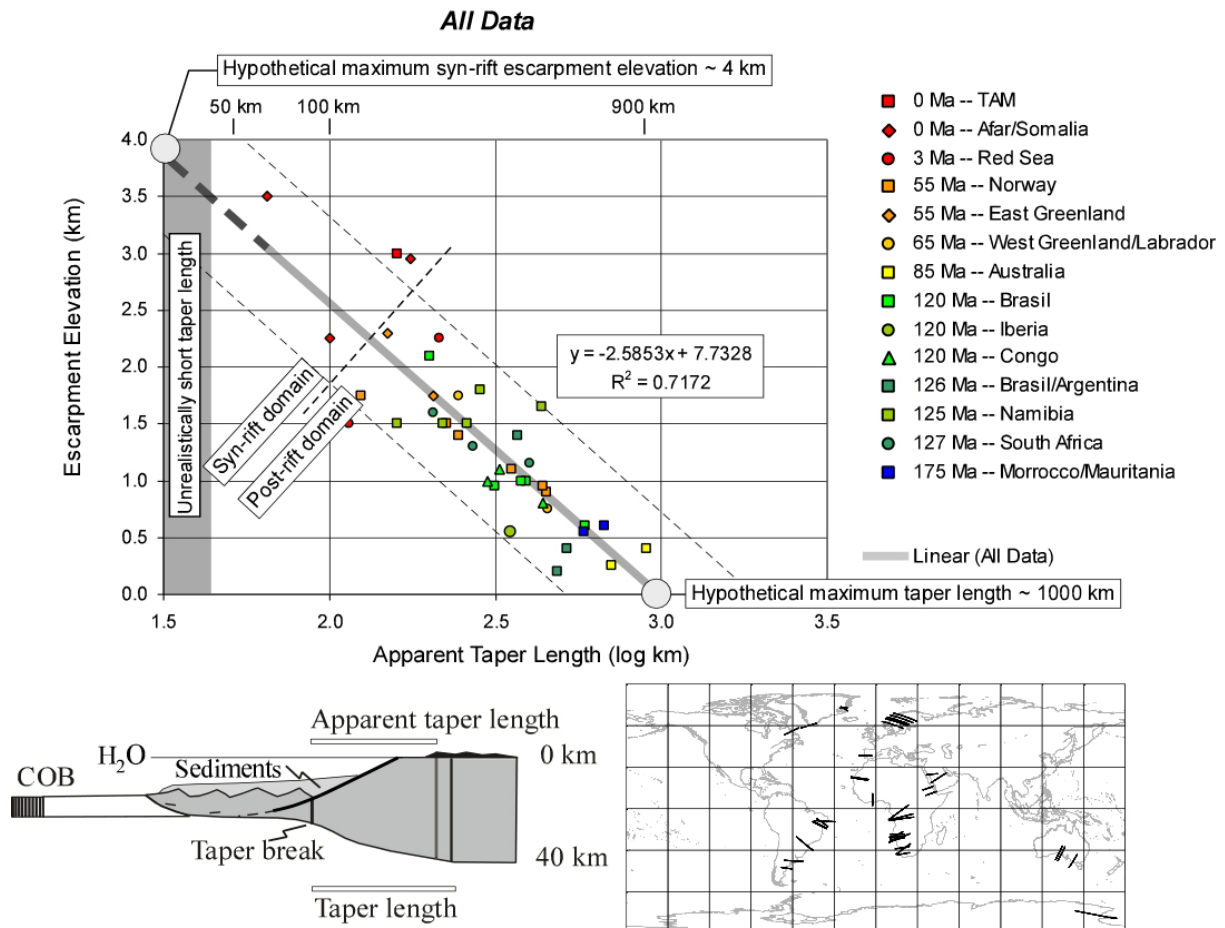


Figure 3.7: Global taper diagram. Relationships between taper and topography determined from 40 deep crustal transects adjacent to 6 rifts, distributed over 8 cratons. The Apparent Taper Length is the horizontal length between the taper break (where brittle crust is thinned to 10 km or less during thinning phase extension; e.g., Manatschal et al., 2001) and the maximum escarpment elevation (which we interpret as a proxy for relatively unthinned continental crust). Large grey dot on the X axis may represent the maximum hypothetical taper length – possibly the farthest point inboard that the effects of crustal extension can penetrate. Large grey dot on the Y axis represents the conceptual maximum elevation of a syn-rift escarpment under a hypothetical tectonic unloading of the crust over a very, very short, distance (e.g., a sharp taper.) The highest extensional escarpment of which we are aware is the Royal Society Range in the essentially syn-rift Transantarctic Mountains, which rises to over 4000 meters. Thus, the taper scaling law appears grounded across a range of observations. *Figure and caption from Osmundsen and Redfield, in press.*

4. GEOLOGICAL HISTORY OF THE MØRE-TRØNDELAG FAULT COMPLEX

The Møre-Trøndelag Fault Complex (MTFC) probably originated in Devonian times, as a principal fault zone related to the transtensional collapse of the Caledonian orogen (e.g. Séranne, 1992; Krabbendam and Dewey, 1998; Osmundsen et al., 2006).

The onshore portion of the MTFC was first defined by satellite image studies (Gabrielsen and Ramberg, 1979; Ramberg et al., 1977; Rindstad and Grønlie, 1986), as a structural zone that extends some 500 km from near Grong in the northeast to near Stad Peninsula in the southwest. Its width is on the order of 50 km.

Ductile to brittle sinistral kinematics characterize the northeastern, onshore end of the MTFC's Hitra-Snåsa Fault (Séranne, 1992; Watts, 2001; Braathen et al., 2002). During Norway's post-Caledonian collapse the MTFC seems likely to have acted as a kinematic link between mid Norway and western Norway (Séranne, 1992; Osmundsen et al., 2006). During this time a large number of regional-scale folds in the Western Gneiss Region north of Stad were formed (Figure 4.1). Their fold axes trend in general NE-SW.

Several studies have specifically addressed the timing of faulting along the Verran and Hitra-Snåsa strands. Grønlie and Roberts (1989) interpreted apparent dextral strike slip duplexes between the Verran and Hitra-Snåsa faults to be of Mesozoic age. Supporting their conclusion, fault-related Mesozoic paleomagnetic overprints have been resolved in several locations along the MTFC (Torsvik et al., 1989; Grønlie and Torsvik, 1989). Grønlie et al. (1994) reported a late Jurassic cooling event along the Verran Fault of the MTFC, recorded by apatite, zircon, and sphene fission track data.

While many of its kinematic records are consistent with strike-slip faulting (admittedly of unknown scale), a significant vertical component has also been reported from kinematic indicators (e.g., Watts, 2001; Redfield et al., 2004, 2005a, b; Osmundsen et al., 2006; Redfield and Osmundsen, 2009). The Hitra-Snåsa strand juxtaposes basement from Mesozoic basin rocks with considerable normal separation (Sommaruga and Bøe, 2002; Grunnaleite and Gabrielsen, 1995), also implying significant vertical throw. Under any interpretation, the MTFC constitutes a long-lived tectonic system.

A regional displacement gradient

Redfield et al. (2005b) interpreted the topography of the MTFC region in terms of an Apatite Fission Track scale normal fault displacement (Figure 4.2). In their model the Great Escarpment is a direct consequence of tectonic rock-column uplift sufficient to offset AFT data at the point of maximum displacement. In a perfect world whose thermal stratigraphy is unperturbed by the effects of paleotopography, the AFT 'age contours' would vary solely with depth. If sufficient throw were to occur across a single large normal fault, a very predictable AFT age pattern should emerge (Figure 4.2 top). As a practical matter, many factors affect both the thermal stratigraphy and the AFT apparent age (see discussion in Redfield, 2010). However, AFT data from the MTFC do illustrate a recognizable version of the expected apparent age pattern (see Figure 3.3; also Hendriks et al., 2007). The displacement gradient model is consistent with the hinterland drainage patterns that are evinced in Scandinavia's physiography; its point of maximum throw is also consistent with the Rule of Taper.

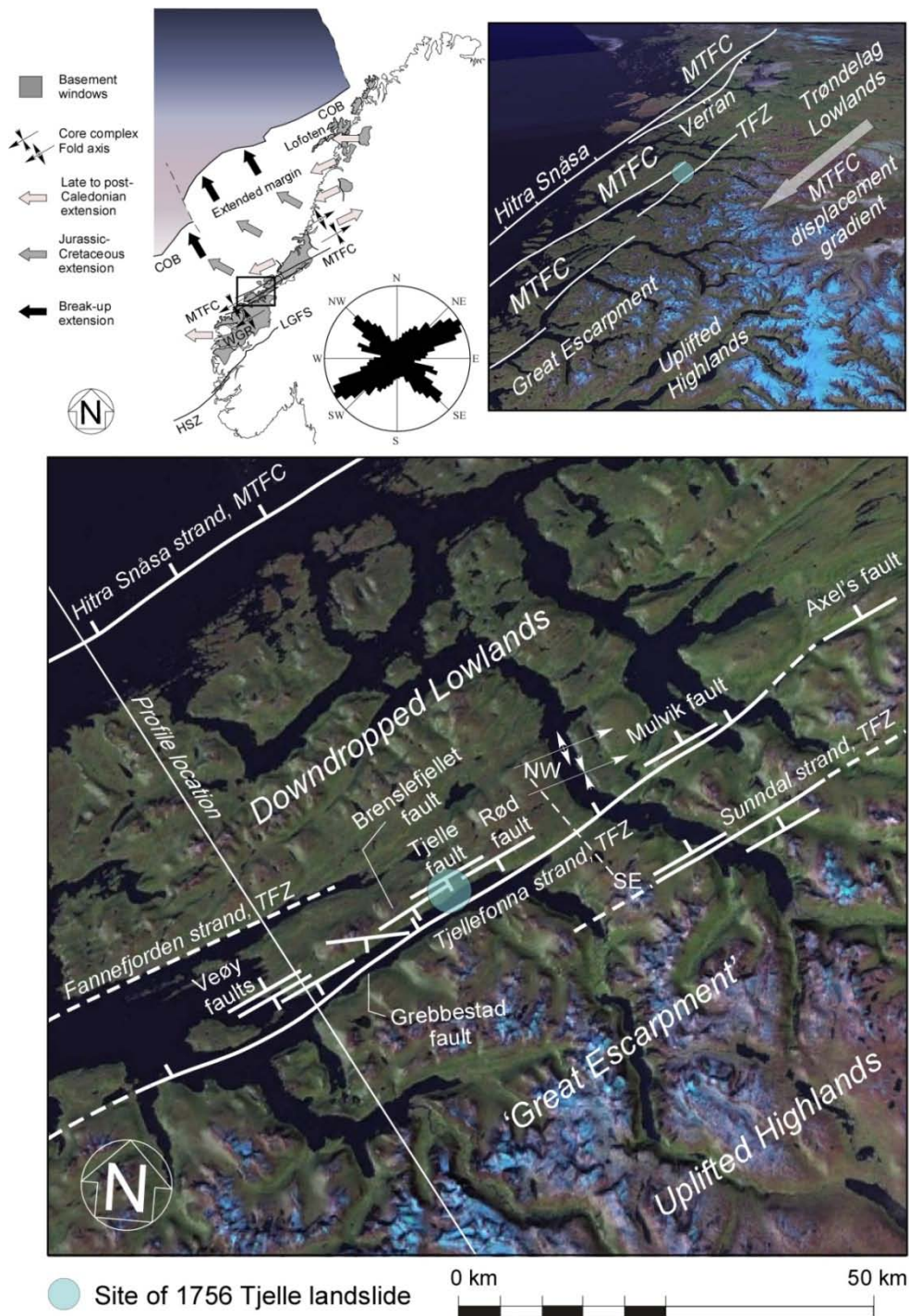


Figure 4.1: Upper left: Extension directions through time. In late Caledonian to post-orogenic collapse time extension was directed to the SW; during this time the MTFC may have acted as a sinistral transfer fault. Block arrows illustrate the changing nature of the principle direction of extension (after Mosar et al., 2002) from post-Caledonian orogenic collapse through Early Tertiary break-up. Box outlines the Langfjord region. MTFC = Møre-Trøndelag Fault Complex. HSZ = Hardangerfjord Shear Zone. LGFS = Lærdal-Gjende Fault System. COB = Continent-Ocean Boundary. Upper right: Oblique image over the MTFC illustrating the gradual rise of topography inboard of and parallel to the main strands of the fault complex. At the upper right of this inset figure, the MTFC retains its older strike-slip kinematic indicators, no statistically significant AFT juxtapositions or topographic contrasts can be observed. Lower figure: At the southwestern end of the MTFC, topographic contrast is considerable and AFT juxtapositions require kilometer scale normal offset (see Redfield et al., 2004, 2005a). The Langfjord region at the base of the Great Escarpment is particularly rich in fault outcrops (symbolized by strike/dip indicators). Arrows depict the orientations of fold axes. Composite images over MTFC and the Langfjorden, courtesy of www.norgei3d.no. See Redfield and Osmundsen (2009).

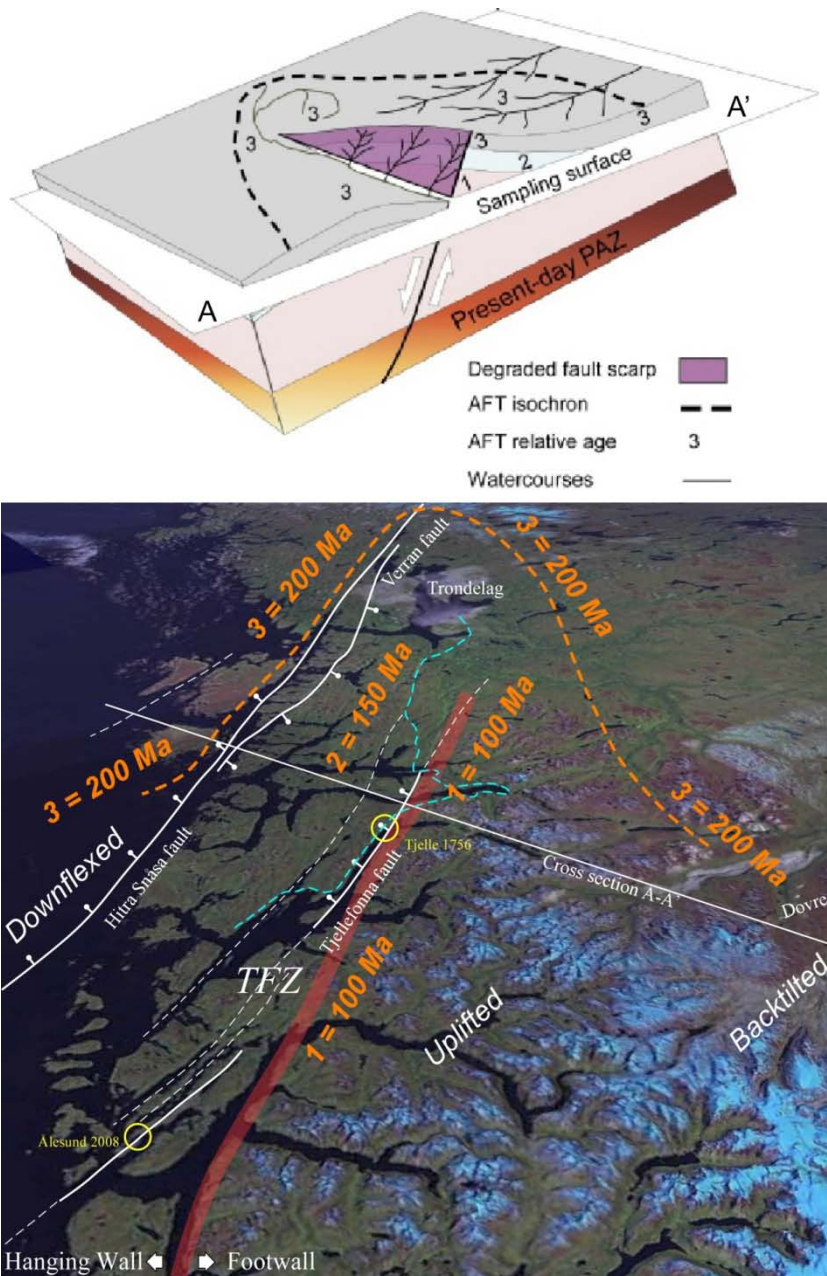


Figure 4.2: Top: conceptual block model of an Apatite Fission Track (AFT) scale normal fault. The apatite Partial Annealing Zone (PAZ) is the region where fission tracks in apatite are partially stable; this is roughly equivalent to a temperature range between 60 and 100°C. An AFT ‘age’ thus represents something between 2 and 4 km depth, with a lot of caveats concerning the rate of cooling, the paleogeotherm, fluid circulation, the original ‘shape’ of the paleo-thermal stratigraphy, radiation damage, and so on (see discussion in Redfield, 2010). The block diagram represents a kilometer-scale perturbation of AFT apparent ages following a normal fault displacement. In this scheme, the relative age increases upwards from age 1 to age 3. Clear apparent age patterns are expected as a function of location with respect to the fault maximum displacement and the fault tip. Bottom: The AFT world as it is in the MTFC. Note how the topography rises to the SW, away from the Trøndelag region. The approximate location of the asymmetric profile of Figure 3.4 is shown by the dashed thin white line. Observed sea-level AFT ages (Figure 3.3) have been grouped into 50 Ma bins; these are equivalent to the relative ages 1-3 of the block model. Orange dashed line indicates the zone of equivalent AFT ‘age’ that encompasses the normal fault displacement - the black dashed line of the block model. Approximate route of the field trip is marked by dashed cyan line. Our transect is right through the heart of the uplifted footwall. See Redfield et al. (2005b) for original discussion of AFT displacement gradient.

Seismicity along the MTFC: As is much of coastal Scandinavia, the MTFC is characterized by low-level seismicity (Figure 4.3). Although magnitudes exceeding $M_w = 5.0$ are recorded, the vast majority of events are closer to $M_w = 2.0$. However, many of the larger events are spatially associated with the southern end of the MTFC. For example, on January 22, 2007, an $M_w 4.0$ tremor occurred onshore near Ålesund, western Norway. Due to the paucity of recording instruments, few focal plane mechanisms are available. From the few that have been computed Hicks et al. (2000) suggested coastal mid Norway in the MTFC region is currently under a transtensive regime (Figure 4.3).

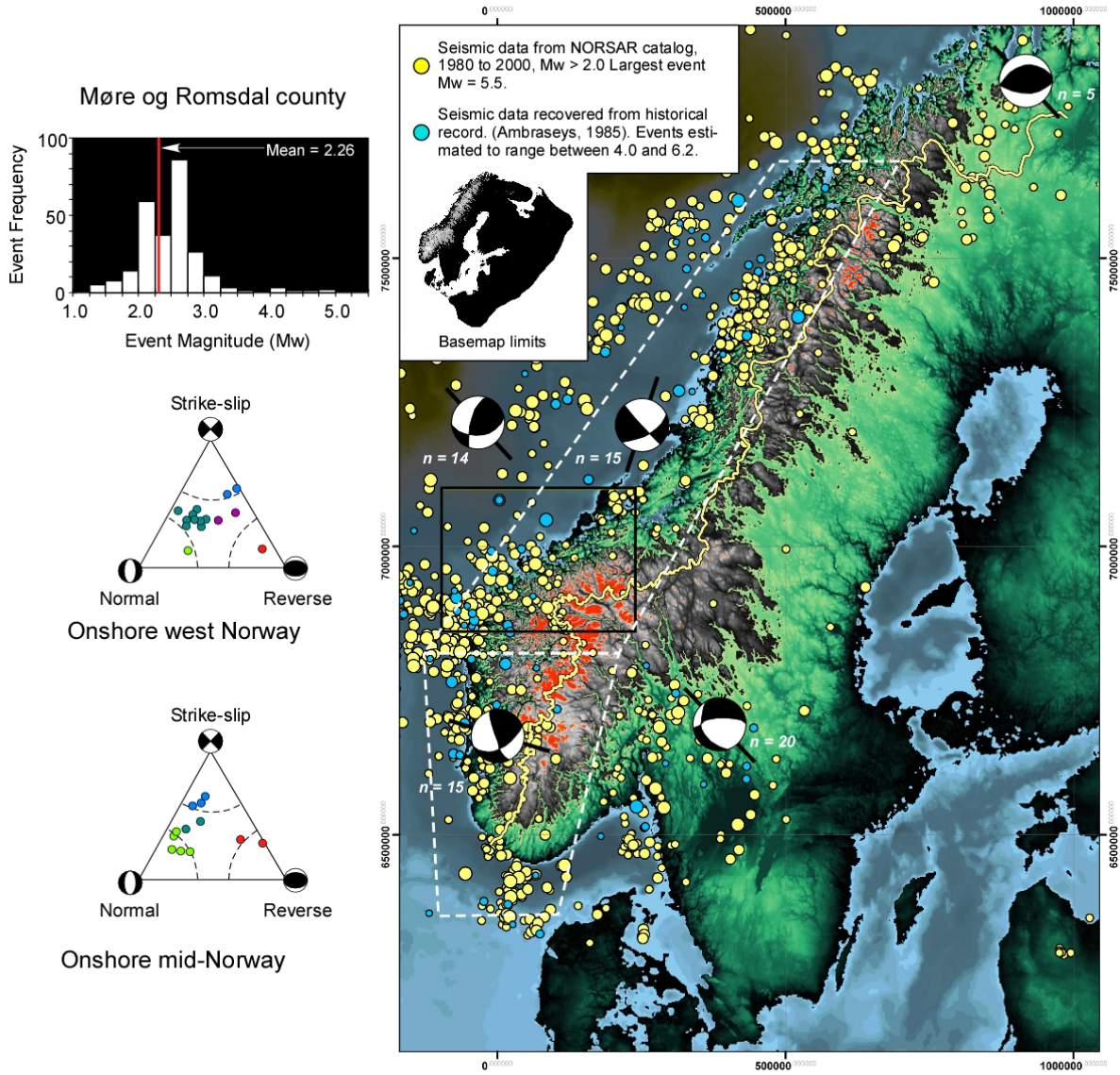


Figure 4.3: Seismic epicenter plot for Scandinavia, showing micro- and macro-seismic events recorded between 1980 and 2000, and events relocated from historical records. The Langfjorden region and much of the MTFC are encompassed in the black box.

Rockslides: On March 26, 2008, a catastrophic rockslide occurred in central Ålesund. There, a well-exposed and steeply-dipping normal fault belonging to the MTFC system slices through the city near the locus of instability. At the rockslide site itself, a steeply-dipping gouge zone, sub-parallel to the well-exposed normal fault, lay beneath fractured blocks (Trygstad, 2002). Though the processes triggering failure at Ålesund were very different than those at Tjelle (Stop 4), the structural template underlying Ålesund is the product of a very similar Caledonian to post-breakup geological history.

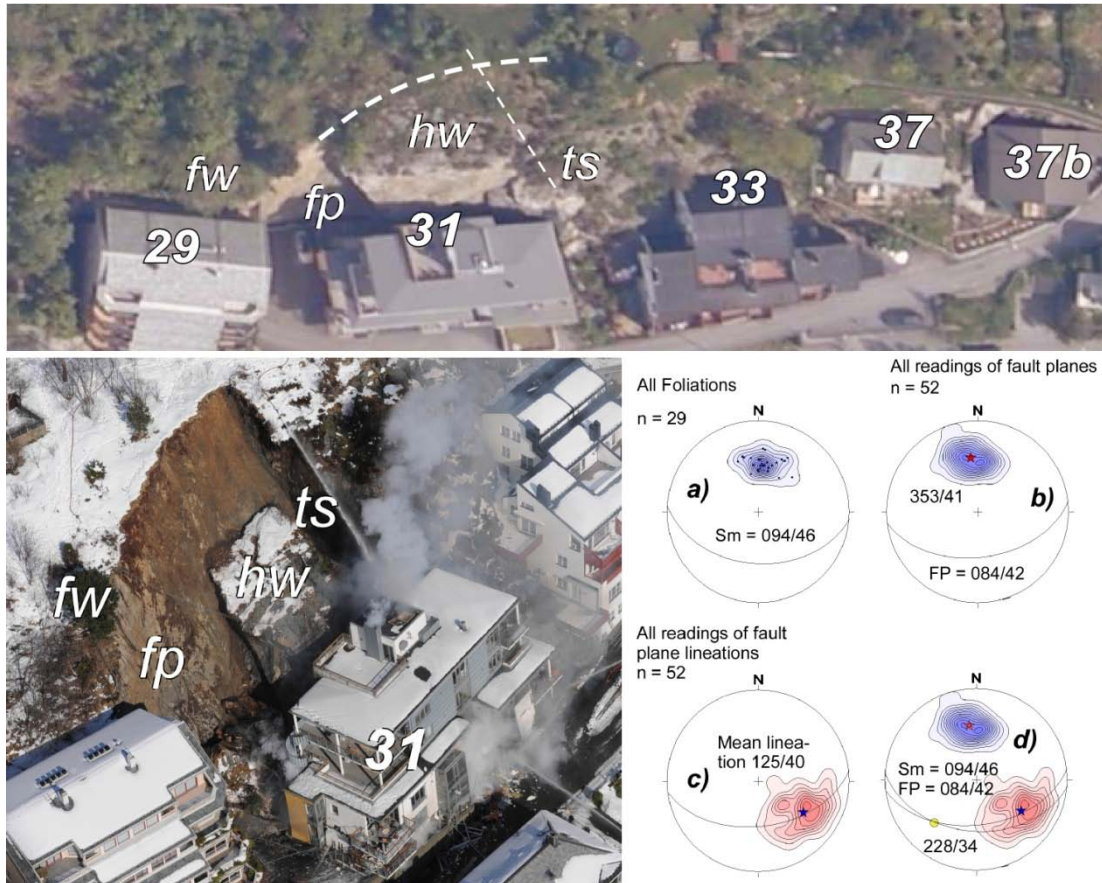


Figure 4.4: Rockslide accident at Fjelltunveien 31, Ålesund. Top panel shows the apartment block (31) prior to the slide. fw = footwall. hw = hanging wall. ts = transfer structure. Heavy dashed line denotes pre-existing normal fault (Trygstad, 2002). Lower left: The hanging wall block failed on March 26, 2008. fp = fault plane. Note reddish patches on fault plane; this is probably the fault gouge reported by Trygstad (2002). Subsequent structural investigation recovered obliquely-plunging mineral slickenlines with normal kinematic indicators (lower right). The fault plane in question belongs to the Tjellefonna Fault Zone within the MTFC system, where the MTFC footwall has achieved its maximum throw (Figure 4.2). Fracture planes, foliation planes, and fault planes conspired to compartmentalize the hanging wall. The instability was augmented during construction when house foundation excavations undercut the toe of the rock body. Failure may have been directly due to freeze-thaw expansion and contraction.

5. FIELD TRIP LOCALITIES

The schedule is based on reasonable driving times, calculated with the aid of a roadmap and Google in the quiet confines of the coffeeroom. How it plays out in reality is another matter. We will attempt to make it back to Trondheim by 20:00, but there is a ferry to catch and all manner of other distractions. So please: when you are requested to *get on the bus*, please do so!

08:00 **Departure** from the parking lot.

We do mean departure at 08:00, not “Let’s all start getting on the bus at 08:00.”

08:15 **Stop 1:** Overlook above Molde

10:00 **Stop 2:** Faults at Vik and Veøy

11:15 **Stop 3:** Rød Fault

12:00 **Stop 4:** Tjelle disaster memorial

12:30-13:00 **Lunch**

13:30 **Stop 5:** Geophysical studies, Eidsøra

15:30 **Stop 6:** Mulvik Fault

17:00 **Return to Trondheim**

20:00 **Arrival in Trondheim**, Rica Nidelven

STOP 1

Molde's Varden overlook (Figure 5.1.1.) provides a panoramic view of Norway's stepped topography and the sharp topographic Great Escarpment. This prominent landmark is heavily incised by alpine glaciers, presenting a strong contrast with the landscapes on either side. It separates high-elevation, low-relief 'paleic' surfaces from low-elevation hilly topography moderate relief (e.g. Etzelmüller et al., 2007, Figure 5.1.2). The topographic envelope between the coast and the Great Escarpment exhibits several pronounced steps. A possible tectonic origin for the 'Great Escarpment' was hinted towards by Holtedahl (1953) and Torske (1972), mentioned by Lidmar-Bergström et al. (2000), and substantiated with AFT and structural data by Redfield et al. (2004, 2005a,b) and Redfield and Osmundsen (2009).

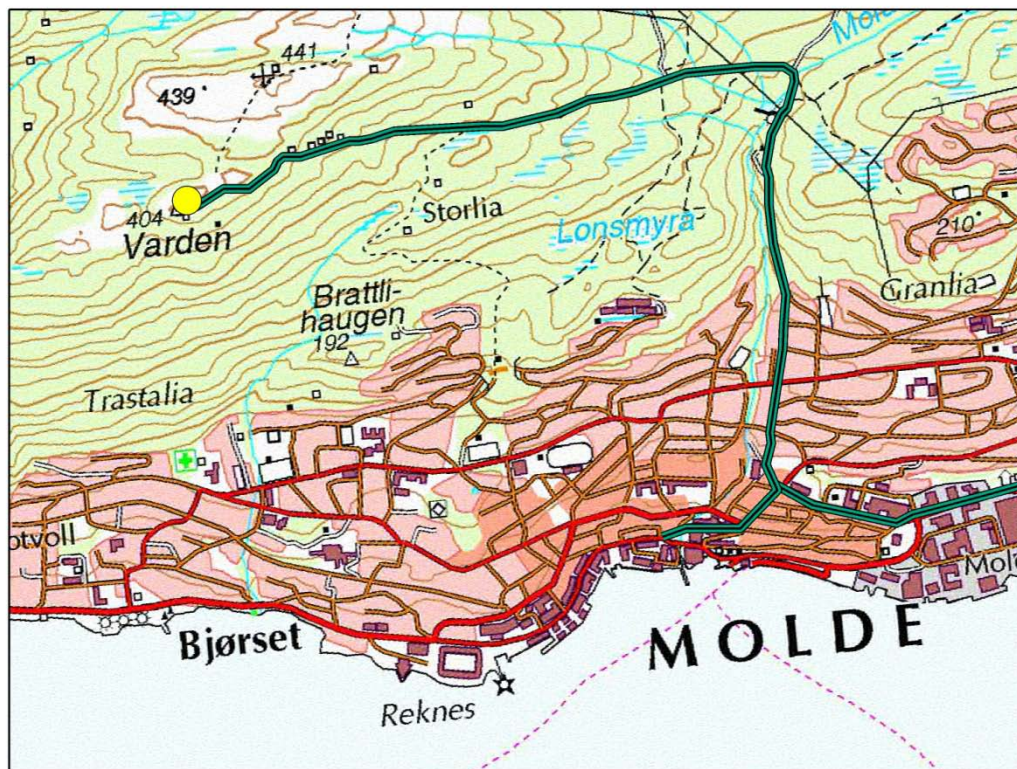


Figure 5.1.1: Location map for Stop 1. The overlook is shown as the yellow dot.

Offshore, interpretation of seismic and potential field data indicates the crustal thinning gradient is extreme (Faleide et al., 2008; Osmundsen and Ebbing, 2008). Onshore, AFT data indicate down-to-the-NW sense of throw at the kilometer scale since at least 90 Ma across the Langfjorden, in accordance with an AFT-scale normal fault displacement gradient along the inner strands of the MTFC (Redfield et al., 2005b).



Figure 5.1.2.: In the event weather is uncooperative (not uncommon in these parts) the above panorama illustrates what we would otherwise have seen. Note the relatively reduced, non-alpine topography adorned by non-glacial landforms in the immediate foreground of the picture. Beyond, the landscape rises in an abrupt yet step-like manner. The Great Escarpment itself forms the distal backdrop, replete with cirques, horns, spires, and arêtes left behind as finishing touches by the Pleistocene ice. On its far side lie other mountains, some even higher; their summits, however, are flattened and at best only lightly incised.

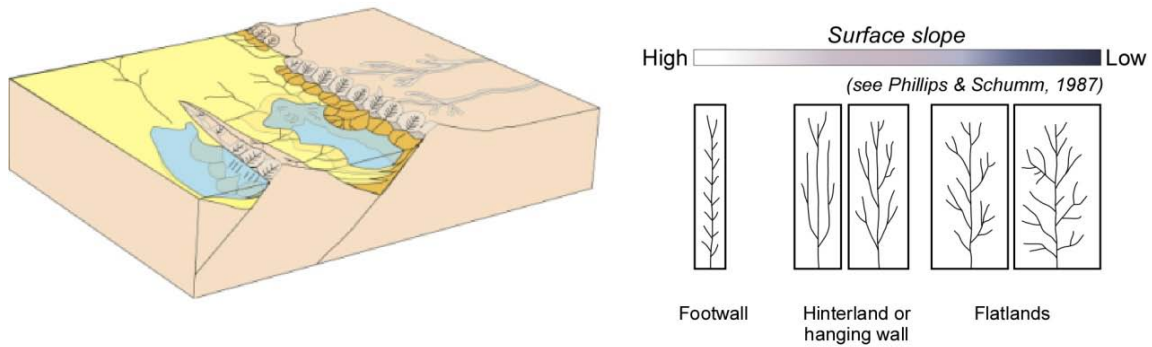
Published AFT apparent ages require a statistically significant difference in cooling history between the alpinized Escarpment and the ground upon which you are standing. For example, a sea-level AFT apparent age on the peninsula near Søsnes Ferry clocks in at 202 Ma \pm 44 Ma (2σ), whilst at Åndalsnes, far in the distance, the sea level AFT ‘apparent’ age is 129 Ma \pm 14 Ma (2σ). In between lies what we think is a big fault in the Langfjorden (Redfield and Osmundsen, 2009). These AFT offsets are not unique. More than 30 AFT age and track length pairs document ‘down to the west’ relative cooling across the MTFC (Figures 3.3 and 3.4; see Redfield et al., 2004, 2005a). Clearly, a statistically significant difference in cooling history exists between the foreground of the picture and its background. This difference holds the key to Norway’s escarpment topography.

The geomorphic contrast between the alpine Great Escarpment (footwall) and the hilly topography we stand on (hanging wall) is rather extreme. We interpret this contrast under the model of Osmundsen et al. (2010), originally developed for the area of Sortlandsundet in northern Norway, but tentatively applicable to other linear alpine ranges in Norway including the Great Escarpment (Figure 5.1.3).

The land between the Great Escarpment and the coast consists of low mountains and valleys, and hills of moderate slopes (Etzelmüller et al., 2007; see Figure 3.5). The degree of ‘alpinization’ is much lower here than in the Great Escarpment. Some of the more planar landforms may be surviving elements of a Cenozoic fluvial erosion surface (Anda, 2011).

Does the extended margin become stronger and less flexible, or weaker with age? This is a question we will not attempt to answer it here (see, for example, Masson et al., 1994; Péron-Pinvidic et al., 2008; Lundin and Doré, 2011). However, it may have a critical impact on the way we understand the landscapes of western Norway.

Pre-glacial: normal faults impose tectonic drainage patterns.



Post-glacial: alpine landforms are preferentially excavated on the footwall.

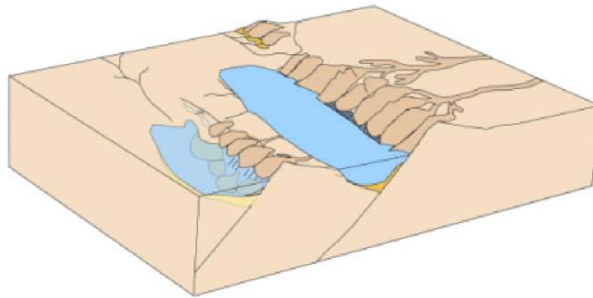


Figure 5.1.3: Above right: observations and experiments show that distinctive drainage patterns develop atop slopes in accordance to gradient (see Phillips and Schumm, 1987). It is well established that across active normal faults, the steep footwall slopes became more densely incised by rivers networks than the more gently dipping surfaces on the hangingwall slopes (e.g. Leeder and Jackson, 1993). For a glaciated fault-block and half-graben, we envisage the following scenario: during repeated glaciations, the most alpine topography evolved in the areas that had the densest configuration of pre-glacial river valleys. Thus, in the footwalls of normal faults, glacial exploitation led to removal by erosion of large portions of the intervalley areas, leaving only arêtes and peaks between U-shaped valleys and cirques. In the hanging walls and hinterland slopes, river valleys were eroded to similar U-shaped profiles, but because of the lower pre-glacial valley density, much larger areas of the paleolandscapes were preserved between them (Osmundsen et al., 2010).

STOP 2

We will cross the Moldefjord by tunnel and bridge and visit several small faults that crop out along the (hopefully sunny) banks of the southern Langfjorden. Several of these were investigated and documented in detail in an NTNU Master Thesis by Bauck (2010).

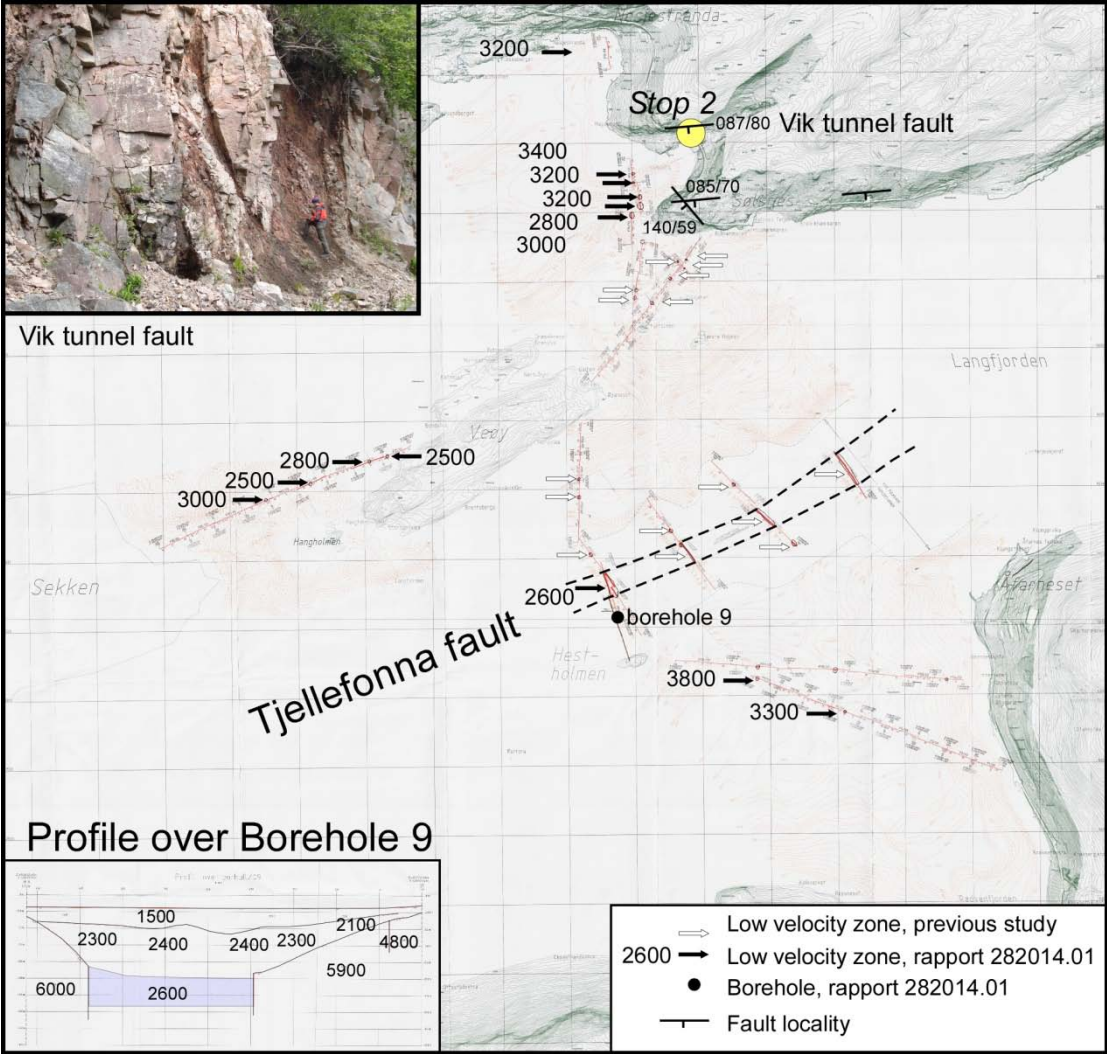


Figure 5.2.1: Location map for Stop 2. The outcrop is shown as the yellow dot. Park about 100 meters before the south entrance to the tunnel, on the NE side of the road. Two smaller faults can also be visited at Søsnes itself if one is waiting for a ferry.

The outcrop by the tunnel at Vik in the western end of Langfjorden (Figure 5.2.1.) displays anastomosing fault planes that define a hierarchy of fault lenses separated by brittle fault rocks. Preliminary borings and seismic refraction data acquired during planning of a subsea tunnel under Langfjorden (Figure 5.2.2) indicate a wide, low-velocity zone under the fjord, typified by extreme fracture densities and unconsolidated (fault) rocks. The faults at Vik, Rød and Mulvik are interpreted as part of the damage zone to the much larger fault that dwells in Langfjorden at the base of the Great Escarpment (Tjellefonna Fault of Redfield and Osmundsen, 2009).

The main tunnel under Langfjorden would be between 10 and 11 kilometers long, and would reach 330 meters below mean sea level, making it the deepest subsea tunnel in the world. In preparation for the project, refraction shallow seismic data were collected (see Statens Vegvesen Rapport 282014.01). In this report, 4000 m/sec is taken as a cutoff value; lower velocities are interpreted as highly fractured rock or otherwise weathered material. Many such low velocity zones were encountered in this study and in previous Statens Vegvesen studies (Figure 5.2.2). A swarm of narrow low-velocity zones lie immediately offshore of the Vik tunnel fault; a string of narrow low-velocity zones follow the main MTFC trend and a strong

topographic edge lineament just SW of Veøy, and a ~200 meter wide ultra-low velocity zone of 2600 m/sec is located in the middle of the Langfjorden, trending exactly parallel to its banks. Borehole core recovery was very poor, indicating extremely unconsolidated rocks were sampled. Given the wet, heavily-fractured nature of the fault rocks documented at Vik, Rød (Stop 3), and Mulvik (Stop 9) by Bauck (2010), the presence of several other similar small faults between Søsnes and Eidsvåg, and a similar geophysical anomaly at Eidsøra (Stop 5), we consider the Langfjorden low velocity zone to mark the trace of the main strand of the Tjellefonna Fault itself.



Modified from Statens Vegvesen Rapport 282014.01

Figure 5.2.2: Map showing results from acoustic profiling in the Langfjorden executed as background preparation for proposed construction of a subsea tunnel. Tunnel route is approximated by the marked seismic lines. Arrow tips indicate low velocity zones (in m/s) encountered in 2009 (black arrows with associated velocities listed in the Statens Vegvesen report) and low velocity zones mapped in previous campaigns (white arrows).

The outcrop at Vik is situated in the AFT apparent age hanging wall (202 Ma +/- 44 Ma at 2σ). The AFT apparent age at Åndalsnes is 129 Ma +/- 14 Ma (2σ). The age contrast occurs sharply, across the trace of the Tjellefonna Fault Zone (see Redfield and Osmundsen, 2009). It is also coincident with a sharp landscape constrast defined by DEM classification analysis (see Etzelmüller et al., 2007). The contrast between both AFT apparent age pairs and

landscape types is consistent with km scale down-to-the-northwest throw across the TFZ (Figure 5.2.3; see also Figure 3.5 and Osmundsen et al., 2010).

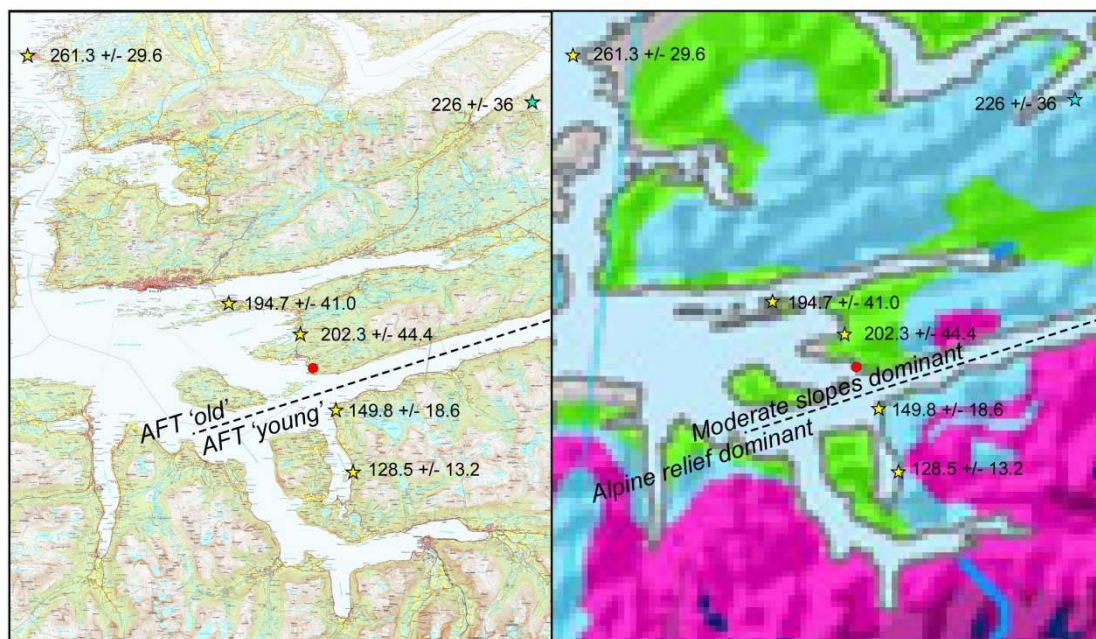


Figure 5.2.3: Vik Fault (Stop 2, shown as a red dot) with respect to near-sea-level AFT apparent ages (yellow stars = data from Redfield and Osmundsen (2009); cyan star = unpublished apparent age by Stiberg (1993)) and DEM landform classes (Etzelmüller et al., 2007). Dashed line depicts the Tjellefonna Fault Zone (TFZ). AFT apparent ages are ‘young’ where the land is heavily excised and ‘alpine’ landforms dominate, and ‘old’ in regions of lower relief and less excised topography. The change in both apparent age and landform style occurs sharply across the trace of the TFZ. This is a similar relationship to that of Sortlandsundet (Osmundsen et al., 2010). AFT error values shown at 2σ .

The main fault plane (Fault 1) has developed a small fault core displayed in picture and line drawing on Figure 5.2.4. Elongated slivers of green cataclasite (a finely-ground fault rock with random internal orientation), clasts of protobreccia, and zeolite minerals occur within it. At least three different generations of zeolite mineralization are present, the last being laumontite. Cataclasite is most likely to form in the elasto-frictional regime, between 5 and 15 km depth (Sibson, 1977).

Zeolites such as laumontite tend to form at shallow crustal depths. For example, in an area with a geothermal gradient of 20 C/km the zeolite facies is at temperatures below 250 C and pressures below 5 kb. However a major fault zone usually has higher heat flow than the surrounding protolith. For example, 35 C/km was suggested for the Verran Fault of the MTFZ by Grønlie, et al. (1991). The zeolites in such a fault zone may form at temperatures up to 300 C and pressures up to 3.5 kb, giving a crustal depth of up to 9 km. Grønlie, et al. (1991) suggested the sequence of zeolite mineralization in the Verran Fault to be early prehnite at 7.5-8 km (250-300°C), laumontite at < 6 km (< 230°C) and ultimately stilbite at 3-4 km (< 170 C). The conditions of zeolite precipitation in the faults studied by Bauck are likely similar. (See discussion and figures in Bauck, 2010).

Bauck's (2010) detailed study of fault kinematics, fault rock compositions, and mineral paragenesis thus indicates the structures at the Vik outcrop were formed during multiple events of normal faulting, under brittle conditions fairly close to the earth's surface.

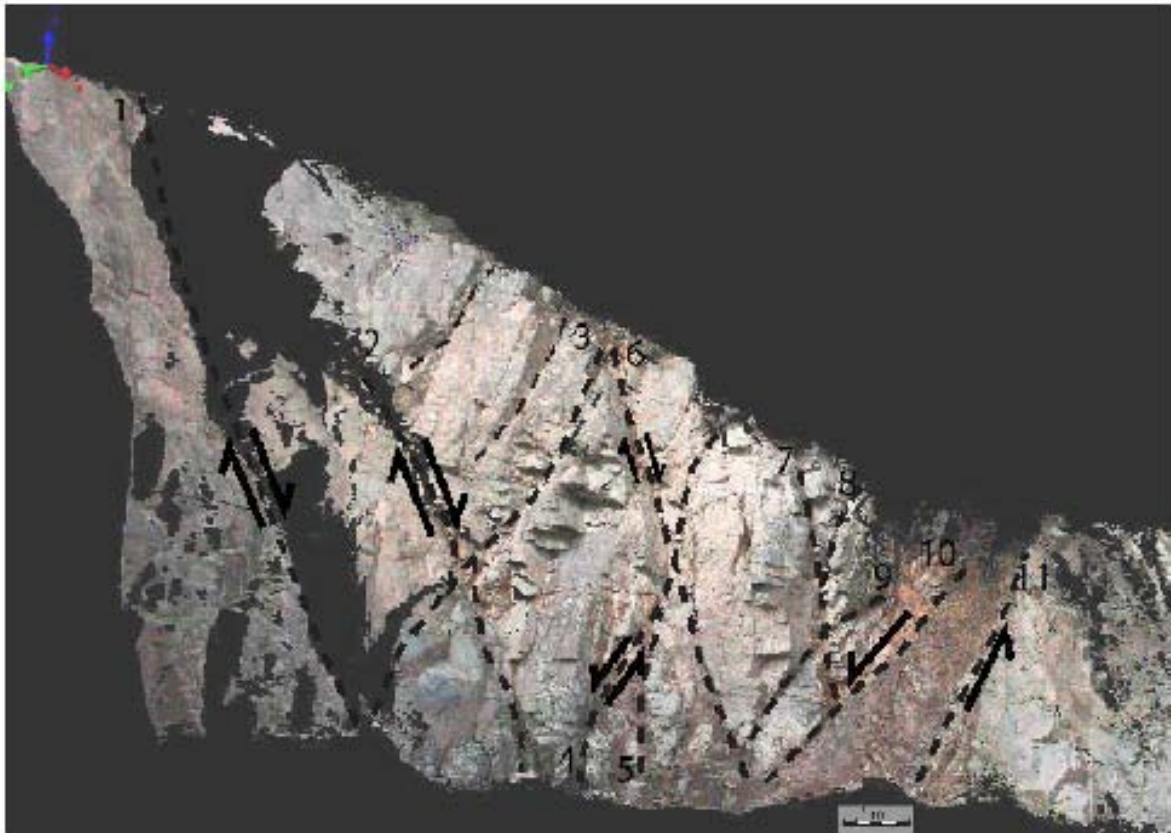


Figure 5.2.4: LIDAR model of Vik Fault showing fault lenses with interpreted sense of shear. The terrestrial LIDAR-scanning was made with the Optech IRIS-3D terrestrial LIDAR scanner. *Figure and caption from Bauck (2010).*

STOP 3

Our travels next take us a short distance to Rød (Figure 5.3.1), where a little fault with quintessentially normal kinematic indicators and a foliation-parallel damage zone is exposed. The Rød Fault was studied by Bauck (2010), in the field, and also by subsequent detailed laboratory work including thin section, SEM and XRD analysis. Fault rocks in the core exhibit evidence for several phases of brittle phase movement and have little cohesion. The core is oriented nearly parallel to the regional foliation, which in turn is oriented near-parallel with the hillside slope.

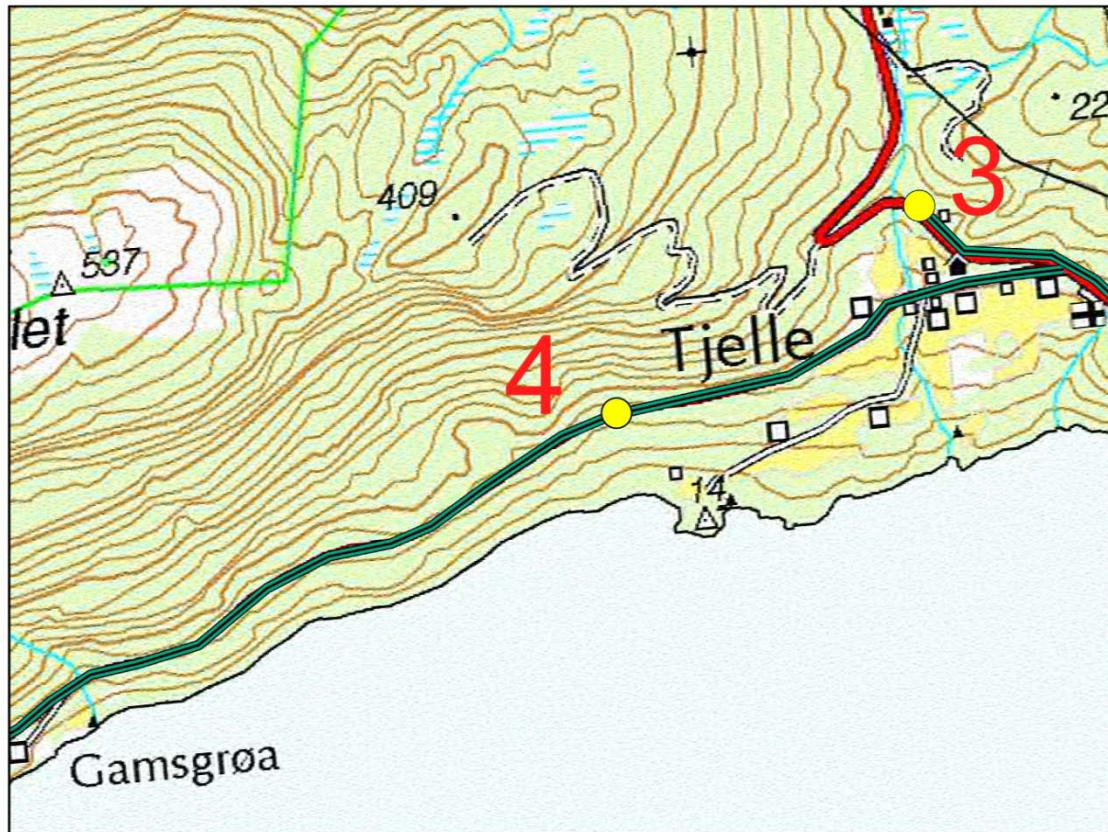


Figure 5.3.1: Location map for Stops 3 and 4. Stop 3: park on the south side of the road, just at the curve. The fault core will be in plain view. Stop 4: parking is at the roadside pullout for the memorial site.

The fault at Rød is a complex structure. Both the hanging wall and the footwall of the main fault plane display well-developed fault lenses. The fault's host rock is classified as granitic gneiss; its core consists almost entirely of altered gneiss saturated by extensional zeolite veins (split arrows on Figure 5.3.2) in E-W direction. The vein mineral (identified as laumontite by Bauck, 2010) seems to be the main component of the breccia matrix. Some zeolite veins cross-cut the breccia. Laumontite is also observed growing in open spaces in the extensional duplexes. This mineral appears to have impregnated the fault core, resulting in a pink to brick colour of the deformed rock.

The main orientation of the fault plane at Rød is $086/66 +58$, displayed as the red great circle of Figure 5.3.2. It is slightly steeper, but sub-parallel to the mean orientation of the foliation, which is $064/49$. In the accompanying rose diagrams, two dominating fracture sets are

evident. One is the trend of foliation and the fault (NE-SW), the other being approximately N-S. The N-S fractures cut and offset the extensional duplex-veins, and are frequently filled with zeolite (Bauck, 2010). High up in the exposure, an intensely-fractured part of the fault core displays fault gouge and crush breccias. These fault products form at very shallow crustal levels (1-4 km depth; Sibson, 1977). Slickenside lineations are found on the main fault plane as well as on small subordinate shear fractures and faults that are associated with it. In the gneisses in the footwall, please note also the older, subhorizontal mineral lineation, a mineral stretching lineation that is probably Devonian in age.

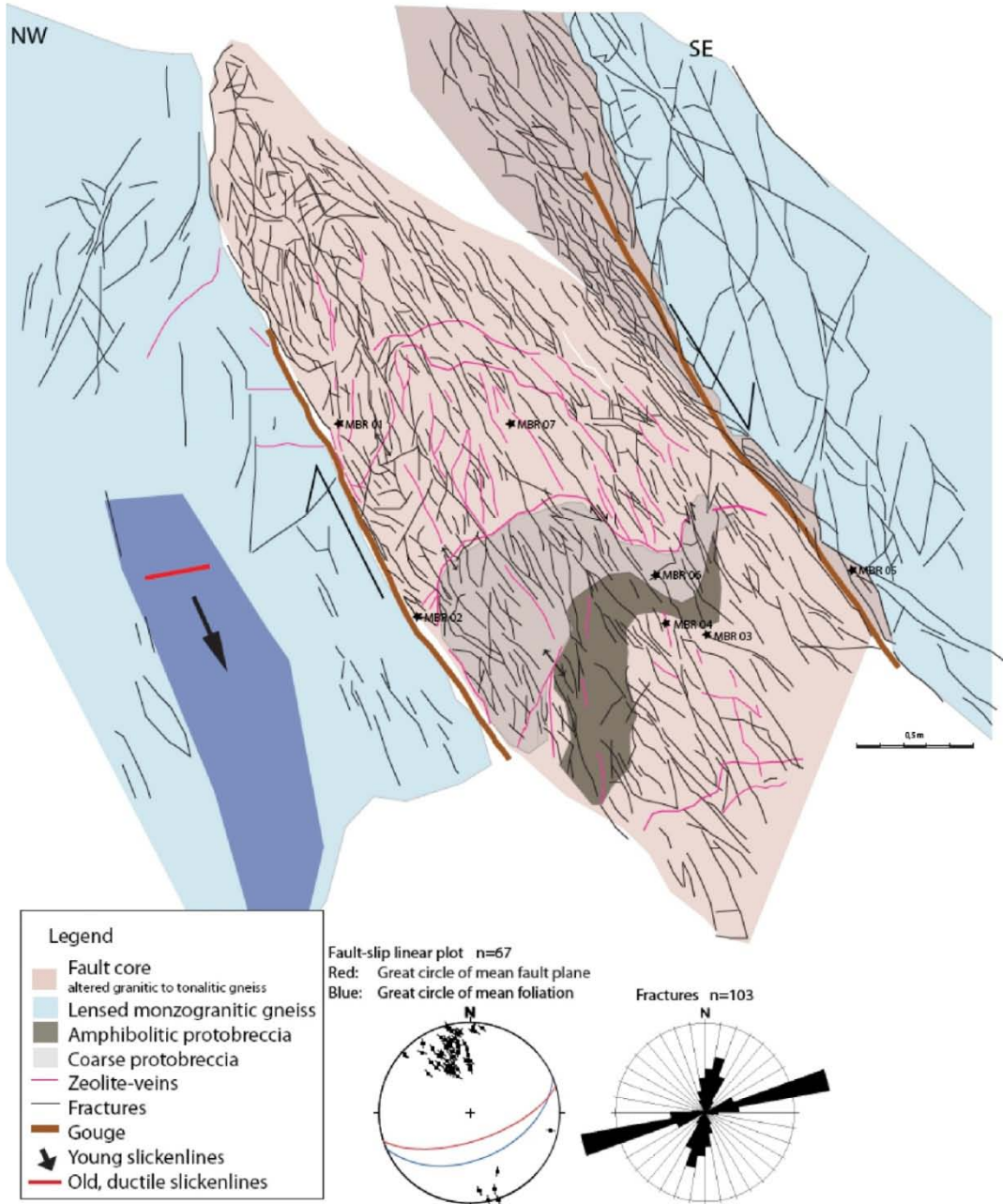


Figure 5.3.2: Line drawing of fault core architecture at Rød showing fault elements mapped by Bauck (2010). Large arrows indicate relative movement. *Figure from Bauck (2010).*

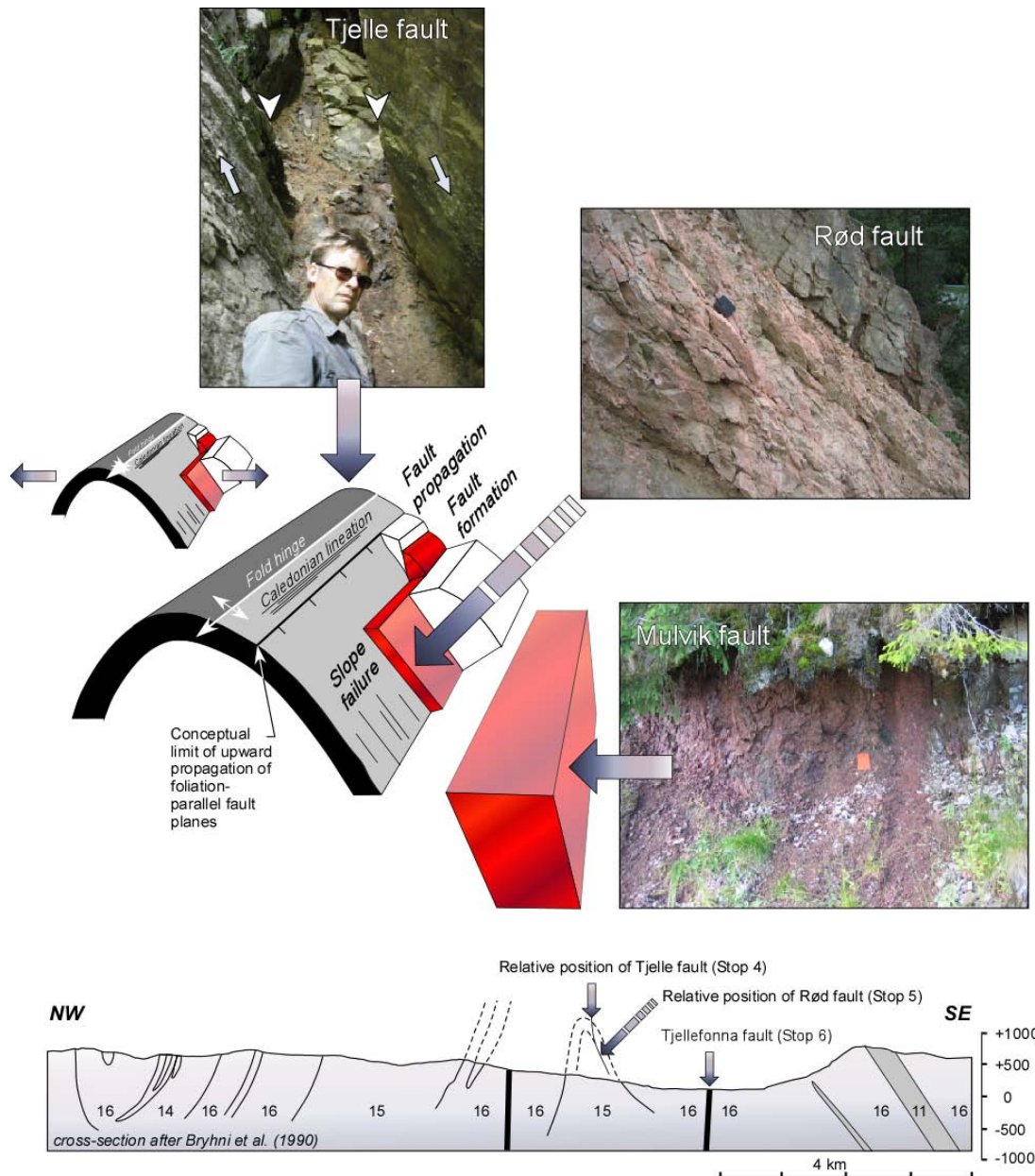


Figure 5.3.3: Photos of normal faults from above the Tjelle rockslide, Rød (nearby to and along strike from Tjelle), and Mulvik, placed in conceptual relationship to one of the fold structures observed parallel to the Langfjorden. The geometry of the Rød Fault, parallel to the regionally folded Caledonian foliation, is interpreted to have formed by Mesozoic or younger reactivation of existing foliation planes.

The relationship between the fault and foliation planes at Rød is instructive. The Rød Fault is situated on the SE dipping limb of a large-scale ductile fold, originally mapped by Bryhni et al. (1990) and part of a regional NE-SW-trending suite of folds that formed under the Devonian constrictional strain field (Krabbendam and Dewey, 1998). Redfield and Osmundsen (2009) suggested that subsequent rifting events placed the limbs of these folds and ductile shear zones that had developed along the limbs under increasing components of tension as the plate motion vector (see Mosar et al., 2002) changed from from SW-NE in the Palaeozoic to NW-SE during the Cenozoic (Figure 5.3.3).

Our next stop will be devoted to exactly this issue. From just down the road, looking back over whence we have come, a prominent scoop-shaped depression can be seen in the skyline (Figure 5.3.4). The scoop marks the site of the 1756 rockslide/tsunami disaster at the village of Tjelle. It also provides a stunning illustration of the second theme to our field trip: normal faults are not only responsible for having built the Great Escarpment of Norway, but they are also actively helping to wear it down.



Figure 5.3.4: View looking towards Rød and Tjelle faults. The Tjelle backscarp can be clearly identified on the skyline. Foliation plane is marked by white arrow. *Figure from Bauck (2010).*

STOP 4

Our stop is at a memorial erected by the local municipality to memorize the victims of the rockslide/tsunami that devastated the village of Tjelle and large areas along Langfjorden in 1756 (see Figure 5.3.1). A fault that appears to have aided the compartmentalization of the now-failed rockslide lies at least an hour's climb up the unstable talus debris, truly well above and beyond the call of duty. However, it shares architectural and fault rock similarities with the faults at Vik and at Rød. Further linkage is plausible; nearby Purka Mountain may also be susceptible to catastrophic failure. It has been speculated that seismically-induced shaking may have caused the already-weakened hillside above Tjelle to fail.

On February 22, 1756, approximately 15.7 million cubic meters of bedrock were catastrophically released as a giant rockslide into the Langfjorden. Subsequently, three ~40 meter high tsunami waves overwhelmed the village of Tjelle and several other local communities. The tsunami killed 32 people, destroyed 168 houses, and sunk 196 boats. Today, Norwegian rural villages are larger, their populations are periodically inflated by tourism, and their town centers, many still growing, are commonly located at fjord level. The Langfjorden region would be devastated should a similar event occur there today.

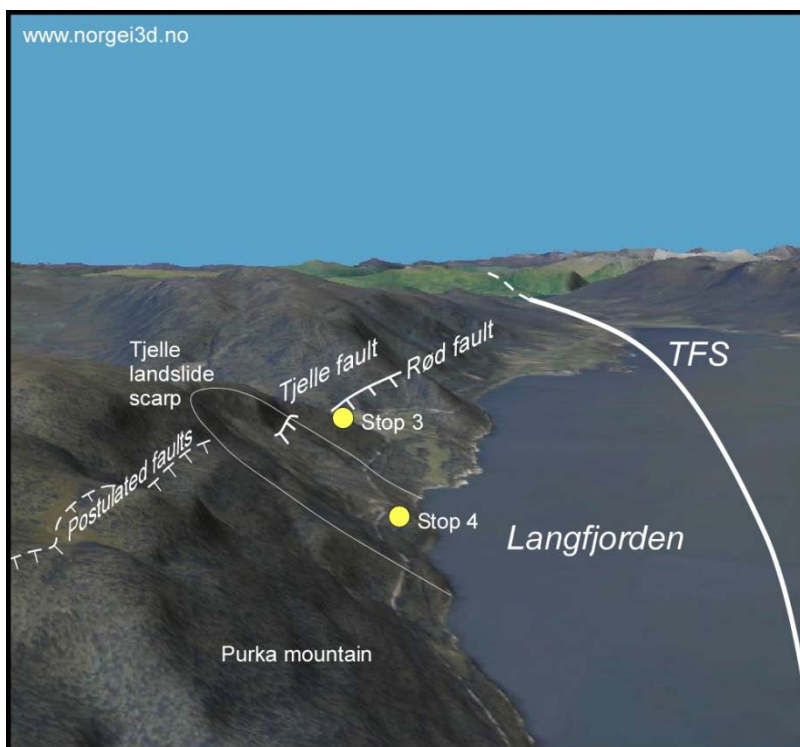


Figure 5.4.1: 3D image (www.norgei3d.no) showing the Tjelle slide scar and the location of the Tjelle normal fault. It is easy to imagine how the traces of the Rød Fault (Stop 3) and the Tjelle Fault (Stop 4) might link. Note the pronounced sag in the upper shoulder of Purka Mountain: it is also easy to imagine how fault linkage might continue across the Tjelle slide scar.

At least one fault core with red cataclasites, zeolite veins and abundant fault lenses crops out at about mid-height in the Tjelle slide scar (Figure 5.3.3). Named the Tjelle Fault by Bauck (2010), it is steeply south-dipping, and sub-parallel to the main hillside gneissic foliation. The Tjelle Fault is directly on strike with a much-more-conveniently-exposed normal fault at Rød (Stop 3), and it is geologically tempting to connect them as linked structures. The geological setting of neighboring Purka Mountain is explicitly similar to that of Tjelle. The structural

geometry potentially favors compartmentalization, and a well-expressed geomorphic shoulder hints of gravitational sag (Figure 5.4.1). Rapidly-growing vegetation in this wet, rain-soaked region² may easily have concealed visible signs of hillside creep. Given these attributes, Purka Mountain would appear to be a good candidate for further study.

The mechanism that actually triggered the Tjelle landslide remains unclear. A week of heavy winter rains is recorded to have preceded the rockslide, and some pre-failure activity may have been observed by local residents in 1755 (Furseth, 2006). Thus, it is plausible that incremental hillside creep along a basal glide plane simply passed a critical threshold. The historical record suggests that other rockslides may have occurred contemporaneously nearby (see the Gazette de France, 10 April, 1756; also Hola, 1976). These citations suggest (though by no means require) that a common trigger could have engendered several slides in Møre og Romsdal county in late February, 1756. Christian Morsing, the vicar in residence in the Langfjorden region, was an eyewitness to the slide and described a long rumbling noise that heralded the event, how household objects were shaken from their places, and, without equivocation, how the disaster was preceded - indeed, *caused* - by a strong earthquake (see Furseth, 2006).

The slope, just by the sea, was not very steep, but had the character of a long slope up from the sea that was covered in grass and trees. From this it is clear that it could not be what in Norway we call 'Fjeldskre' [*rockslide; translators comment*], which tend to happen in the summer, during a long period of hot weather and rain in mountains that are high and steep and have cracks in them and that are without forest, trees, and grass. Because here [*at Tjelle, in the Langfjorden; translator's comment*] the collapse of the mountain must not have happened if it had it not been preceded by an earthquake, because this mountain was of a different situation.

C. Morsing, 1757³; Translated from the Danish by the Authors

Without question, 15 million cubic meters of rock rumbling down a steep hillside must sound a lot like an earthquake. However, the seismic nature of western margin of Fennoscandia is well known (Ambraseys, 1985; Bungum et al., 1979). Many earthquakes of up to magnitude $M_w = 5.2$ have occurred between Måløy (south of Møre og Romsdal County) to points north of Lofoten (Hicks et al., 2000; see Figure 4.3). The nearest-shore to onshore focal plane solutions in this zone are oblique-normal (see Hicks et al., 2000). Between 1980 and 2002, 10 events greater than magnitude $M_w = 2.0$ occurred within 30 km of Tjelle. The seismic event with a focal plane solution that lies closest to Tjelle was recorded in 1996 as magnitude $M_w = 2.8$ with oblique-normal throw (see Tvedt et al., 2002). And on January 22, 2007, an $M_w 4.0$ tremor occurred onshore near Ålesund, western Norway, along the southern terminus of the MTFC.

² Given the cloudless skies and the outrageously warm sunshine under which we are basking, one would never suspect Langfjorden to be a blue spot on the rain map. But it is!

³ Christial Morsing's account contains a lot of interesting material. Beyond his description of the earthquake, his history of the wave-washed evening contains the account of a young village wife and her husband, several tubs-worth of whitefish cast up on the shore, and a fascinatingly-effective local remedy for hypothermia consisting of akavit blended with gunpowder. The young village wife gave birth to a son after having been taken catered in this way by the local farmers who found her among the debris in the early morning after the slide. See Furseth (2006) for details.

Although it is impossible today to prove that the Tjellefonna or nearby faults of the MTFC ruptured in 1756, we (like the vicar) consider it reasonable to speculate that in a faulted, rain-soaked region a seismic event could have caused the already-weakened Tjelle hillside to fail. The Geological Survey of Norway has an active rockslide/tsunami research group that will be supervising a future MS project on the Tjelle event; we anticipate new data will provide more information covering the nature of the instability and its release.

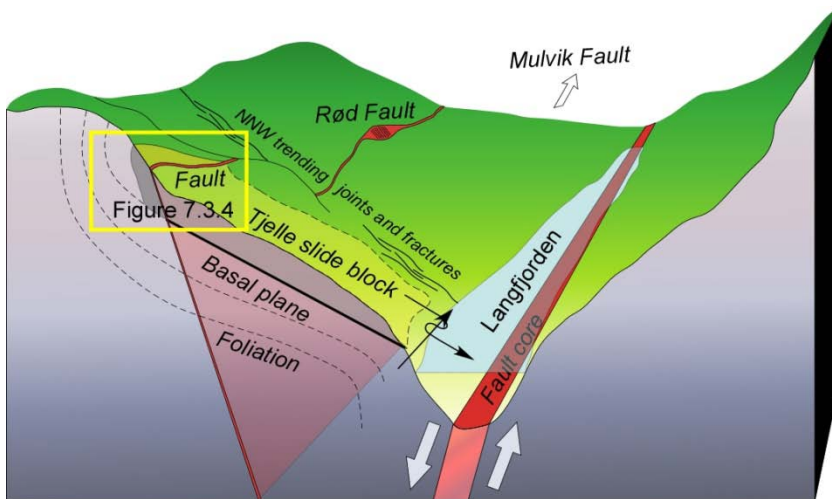


Figure 5.4.2: Block model showing the location of the Tjelle slide normal fault (yellow box) and its hypothesized geometric relationship with the faults at Rød (Stop 4) and in the Langfjorden. Note that the Tjelle slide block may have been isolated along its sides by pervasive regional fractures and at its base by the hillside-dipping regional foliation. See Redfield and Osmundsen (2009).

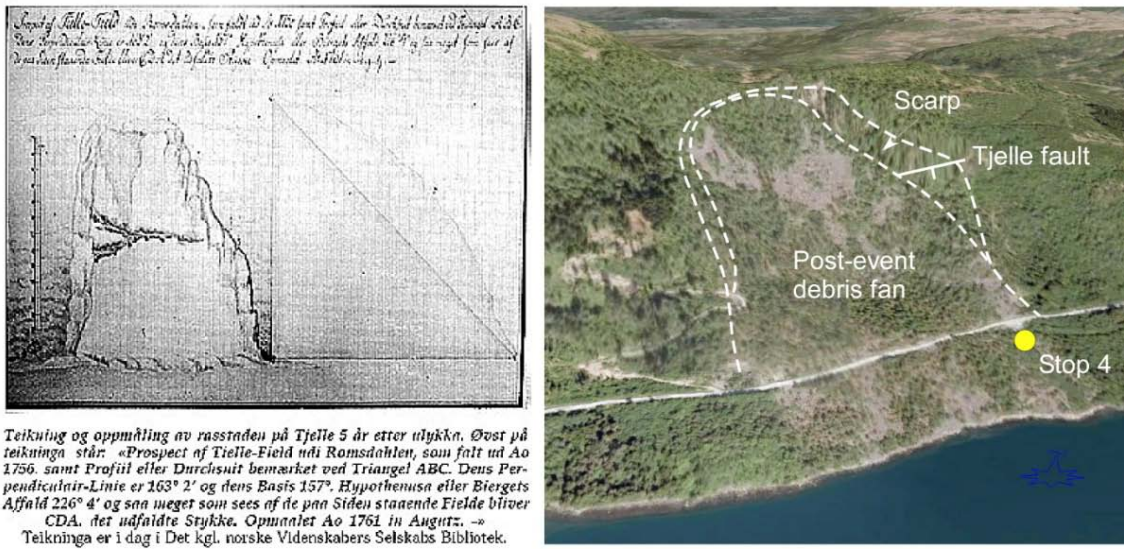


Figure 5.4.3: Left: Drawing and interpretation of the Tjelle rockslide made by an unknown author about 5 years after the disaster. Note the pronounced fault-like feature crossing the slide scar at mid-height. *Det Konglige Norsk Videnskabers Selskabs Bibliotek*. Right: 3D image showing an overview of the Tjelle slide from a similar viewpoint as our Unknown Artist's. The approximate location of the Tjelle Fault outcrop is shown as a strike/dip symbol. From www.norgei3d.no.

STOP 5

At Eidsvåg, a geophysical discourse awaits (Figure 5.5.1). Along Eidsfjorden, experiments using shallow seismic refraction, resistivity, and magnetic data have resolved geophysical anomalies that can best be interpreted as the heavily fractured, wet rock typical of brittle fault zones. The low-velocity zone is on-strike with a similarly-wide low-velocity zone at the southern end of the Langfjorden (Stop 2), also interpreted to document highly shattered, fractured rock in the core of a major fault system. The fault outcrops we have visited at Vik and Rød are interpreted to be part of its hanging-wall damage zone. In 2007 and 2008 a series of gravity, magnetic, 2D resistivity, shallow refraction and reflection seismic profiles were measured across two non-submerged projected traces of the Tjellefonna Fault segment of the MTFC (Figure 5.5.2; see Nasuti et al., 2009, 2010). The aim of the experiments was to locate possible segments of the fault zone and to study their structural attributes. Results from the reflection seismic are being processed at the University of Uppsala as part of a separate project; so far, the data have provided neither confirmation nor negation of the existence of the Tjellefonna Fault Zone. However, the other data sets have provided interpretable results (Figure 5.5.3).

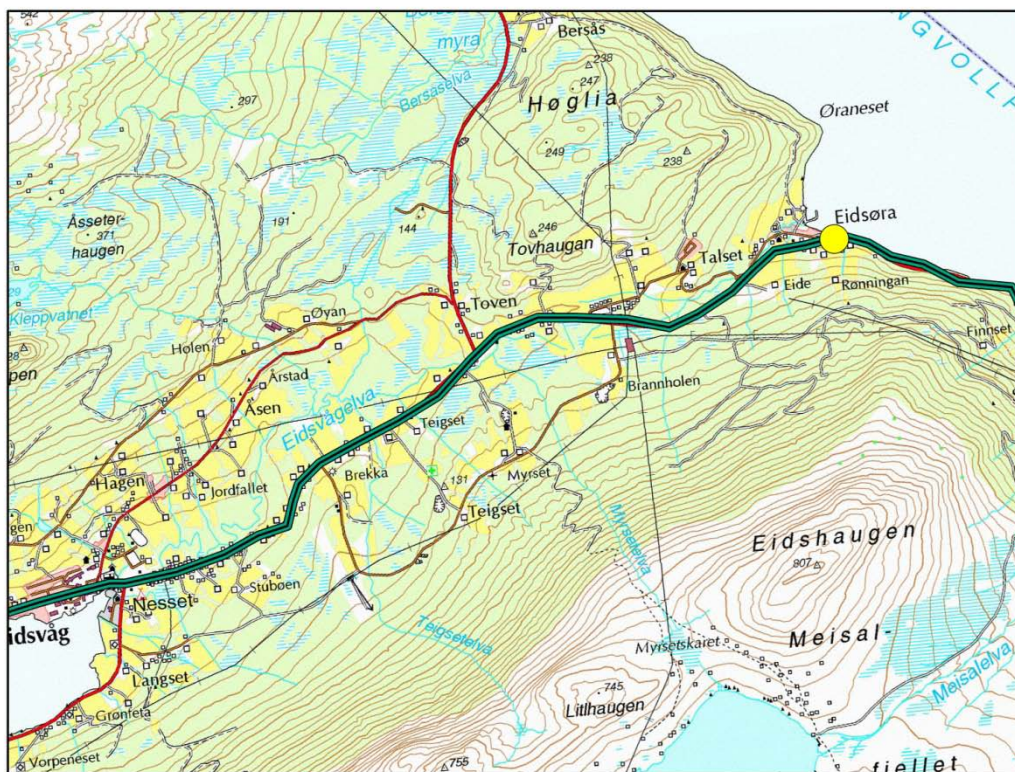


Figure 5.5.1: Location map for Stop 5. The yellow dot marks the location of some of the geophysical profiles; the actual field trip site may be somewhere else nearby. The figures and much text for this stop are taken from Nasuti et al. (2011), where more detailed information can be found.

Figure 5.5.3 shows the results from three independent data sets acquired across the projected trace of the Tjellefonna Fault at Eidsvåg. The top panel shows results from shallow seismic refraction conducted during autumn 2007. A thin layer of soil with very low seismic P-wave velocities (400-600 m/s) was imaged. Just below this layer P-wave velocities increase to

1400-2300 m/s in what is interpreted to be the Quaternary overburden. The underlying bedrock typically exhibits velocities of 4500-5100 m/s but clearly shows three distinctive near-vertical low-velocity zones. Low-velocity zone S2 appears to be wider than S1 and S3 and exhibits 2500 m/s whilst the two other velocity anomalies clock in at 3500 and 3700 m/s. Because low P-wave velocity values (i.e., less than 4000 m/s) are generally indicative of areas of wet, fractured rock, the refraction results are consistent with a large fault core composed of densely fractured rock and/or fault gouge (see also Stop 2).

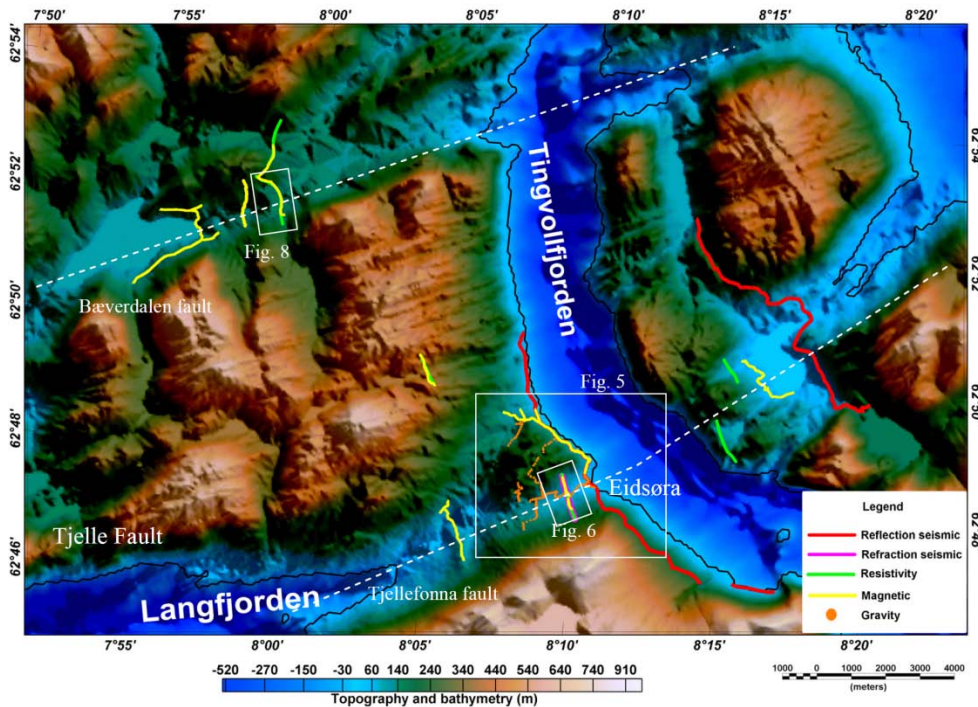


Figure 5.5.2: Location of geophysical data acquisition near Eidsøra superimposed on a shaded DEM image. The respective locations of the different geophysical profiles are shown. The white boxes outline some of the geophysical profiles shown in Figures 5, 6 and 8 of Nasuti et al. (2011) and in Figure 5.5.3.

The middle panel of Figure 5.5.3 shows results from a 1400 m long resistivity profile acquired at almost identical location as the refraction seismic profile. A low resistance top layer corresponds to the top low velocity layer and is interpreted to represent unconsolidated Quaternary sediments. Low resistance anomalies were also imaged in the underlying bedrock (R1, R2 and R3). A very good spatial correlation exists between refraction/resistivity anomaly pairs S2 and R2, and between S3 and R3. As well, respective widths of S2 and R2 are very similar. No visible counterpart is found for seismic anomaly S1. This latter seismic anomaly may potentially be a blind zone and, therefore, may not represent any actual fault zone. In turn, R1 might represent a relatively minor deformation zone.

Three magnetic anomalies depicted as central lows between high-amplitude and mainly short-wavelength peaks were distinguished (i.e., M1, M2 and M3, Figure 5.5.3) along the same profile. (Because of the presence of a high voltage power line, the magnetic profile contains a small gap of ~100m). M2 is the most pronounced magnetic anomaly and correlates very well with refraction/resistivity anomaly pairs S2 and R2. Contacts between rocks with contrasting magnetic properties are commonly associated with positive and negative magnetic anomalies with steep gradients. The M2 anomaly may be caused by contacts between rock bodies of different magnetic properties located at two outer boundaries of the interpreted fault core.

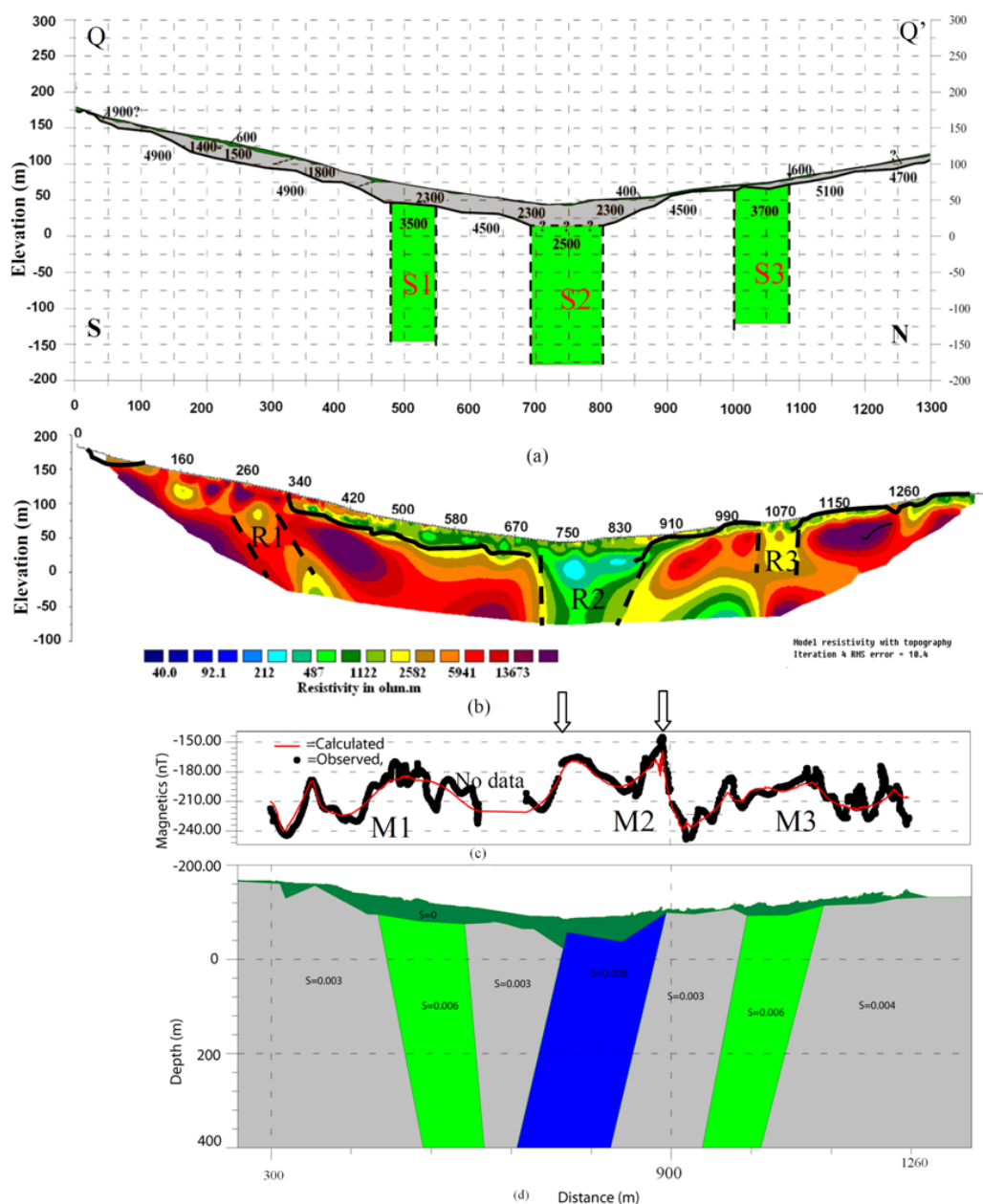


Figure 5.5.3: Geophysical profiling across the Tjellefonna Fault (indicated as Fig. 6 in Figure 5.5.2). (a) The refraction seismic profile shows three low-velocity zones (S1, S2 and S3); velocities in m/s. (b) Depth-inverted 2D resistivity profile showing three low-resistivity zones (R1, R2 and R3). Continuous and dashed lines represent the interpreted top bedrock and the edges of the interpreted main fault zone respectively. (c) Magnetic profile. The arrows on top of the magnetic anomaly show the edges of the interpreted main fault zone. Profile locations are shown in Figs. 3 and 5. (d) Model proposed for the magnetic anomalies.

The model proposed for the magnetic anomaly (Figure 5.5.3) shows three zones with higher susceptibility which could be related to a fault zone in which alteration has led to higher magnetization. In the model the main fault is related to magnetic anomaly M2, which is nearly vertical and slightly dips toward the south. However, it is important to remember that the model purports to explain only the geometry of the magnetic bodies, which are not necessarily the same as the fault core. Furthermore, in a very steep fault zone the difference of just a few degrees will change the ‘geometry’ from normal to reverse, even though the structure is in

reality an anastomosing maze of lenses and damaged rock. Thus, the south-dipping geometry suggested by the magnetic model do not necessarily reflect the overall geometry of the Tjellefonna Fault itself.

In summary, the existence and location of the proposed Tjellefonna Fault is strongly supported by our geophysical data. The data indicate a master fault (i.e., the Tjellefonna Fault coincident with anomalies S2, R2 and M2) in the centre of Eidsøra valley is bracketed by two less-intensively-developed damage zones, and a secondary fault less than 1 km further north (not discussed here). The core of the master fault is ~100-200 m wide and filled with water and/or clay minerals, hence presumably fault gouge and highly fractured rocks. The geophysical structure of the Tjellefonna Fault appears to be nearly identical to that imaged by Statens Vegvesen (Stop 2). Its geological character may share many similarities with the faults at Vik, Tjelle, and Rød (Stops 2, 3, and 4), and perhaps especially with the larger fault core exposed at Mulvik (Stop 9) some 10 km northeast of Eidsøra (see data and discussion in Bauck, 2010).

STOP 6

Our trip will come to a close at Mulvik (Figure 5.6.1), where another fine fault core awaits us, *almost* (geologically speaking) disrobed. The Mulvik Fault exposure contains many small fault cores, and one large one. The topographic and landscape juxtaposition across its trace and its AFT apparent age offsets indicate down-to-the-northwest sense of shear (Figure 5.6.2). Although probably not connected directly to the Langfjorden's Tjellefonna Fault, the Mulvik Fault is part of a linked series of faults we have named the Tjellefonna Fault Zone (TFZ). The TFZ extends from Ålesund to north of Sunndalsøra, and is the innermost architectural element of the Møre-Trøndelag Fault Complex (MTFC).

The Mulvik Fault is a long-lived structure whose fault rocks document multiple periods of activity in the brittle regime, and incorporate fault rock clasts from relatively deep crustal conditions. The fault zone has a significant width: faulted rocks interspersed with relatively intact gneiss occur over an approximately 140 m interval. The fault outcrop exhibits the transition from pure granodioritic gneiss through highly fractured and lensed gneiss, and its further development into proto-breccia and a rich assemblage of fault rocks in the fault core zones.

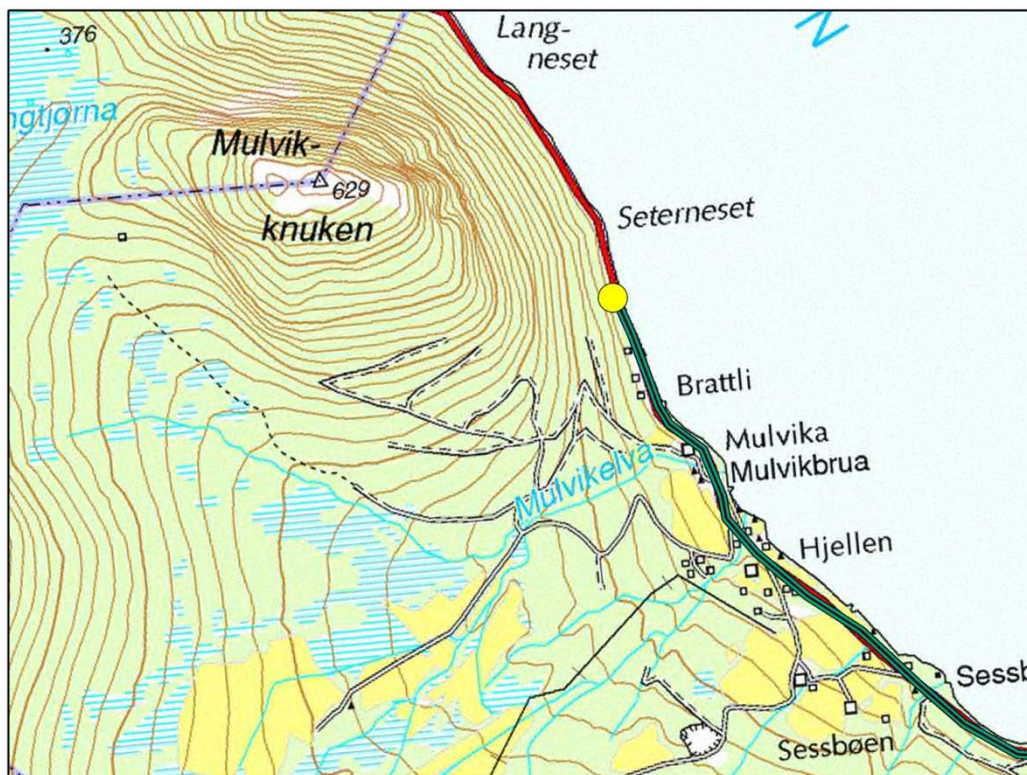


Figure 5.6.1: Location map for Stop 9. A large roadside pullout on the right side of the road in a northwest-bound direction provides easy parking. From there, walk southeast some two hundred meters. Various fault cores are exposed along this roadcut.

Bauck (2010) mapped the Mulvik outcrop in extensive detail, employing also a variety of analytical methods including SEM and XRD. The orientation of the Mulvik Faults described by Bauck (2010) are A) the northern fault of 282/86, B) the southern fault of 252/82 and C) the Mulvik Fault core of 250/80. They have a generally steep, but northerly dip, as indicated

by the northern and southern faults and the near-vertical main fault core. In the slip-linear plot shown in the lower part of Figure 5.6.3, the fault measurements are shown. They show indications of a dip-slip movement of the fault. Geometries and plunge measurements indicate that this is a normal dip-slip fault, albeit the fault is so steep that ‘north side down’ may be a better way to describe it. This is consistent with the sense of AFT offset (see Figure 5.6.2 and Figures 3.3-3.4).

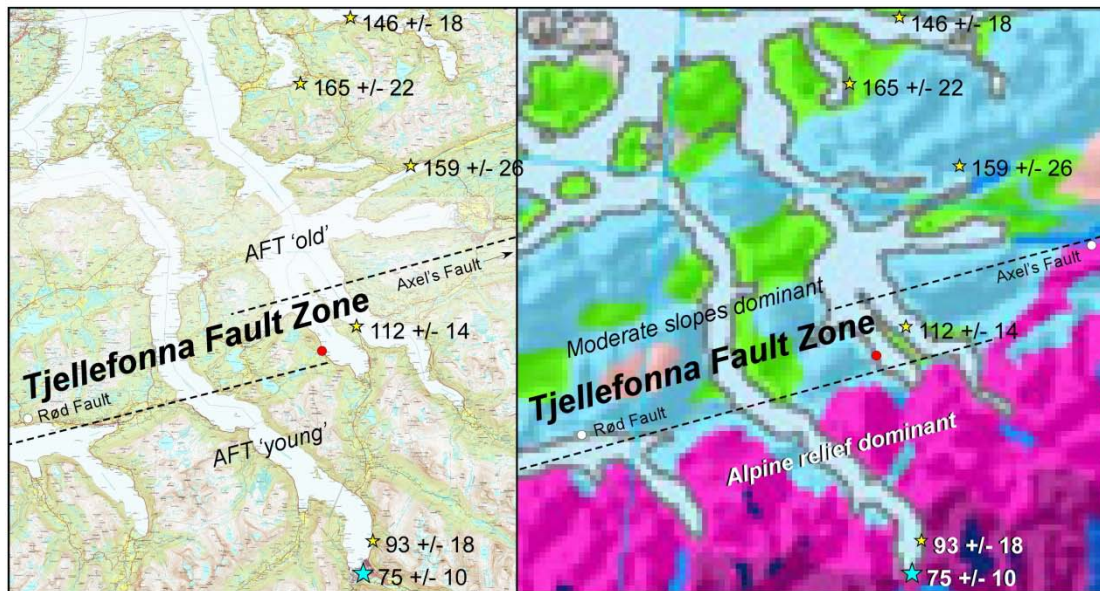


Figure 5.6.2: Mulvik Fault (shown as a red dot) with respect to near-sea-level AFT apparent ages (yellow stars = data from Redfield et al. (2004); cyan star = unpublished apparent age by Stiberg (1993)) and DEM landform classes (Etzelmüller et al., 2007). Dashed line depicts the Tjellefonna Fault Zone (TFZ). AFT apparent ages are ‘young’ where the land is heavily excised and ‘alpine’ landforms dominate, and ‘old’ in regions of lower relief and less excised topography. The change in both apparent age and landform style occurs sharply across the trace of the TFZ. This is a similar relationship to that of Sortlandsundet (Osmundsen et al., 2010). AFT error values shown at 2σ . White dot shows location of the Rød Fault. Dashed lines conceptually represent a fault relay as opposed to actual fault traces *sensu stricto*. Compare with Figure 5.2.3.

Bauck (2010) divided the main Mulvik core into 21 zones (Figure 5.6.3). Its fault rocks record a long and complicated history. Remnants of a fine-grained and opaque fault rock, most likely a pseudotachylite (glass to devitrified glass formed under dry seismic slip or at the base of a rockslide) or ultra-cataclasite (cataclasis involves brittle reduction of mineral-grains, rotation of fragments and frictional grain-boundary gliding and dilation), are found as fragments in MB 05 and MB 08 and MB 12 from Mulvik. More analytical work is required to determine if they are pseudotachylites or ultracataclasites. They represent an earlier phase of faulting than the host breccia. Bauck (2010) suggested that eight events can possibly be recognized. The first two are documented by pseudotachylite and ultracataclasite. Event (3) is documented by cataclasite, possibly representing sinistral transtension from Permo-Carboniferous activity. The next event (4) is a set of zeolite mineralizations, thought to be from the post-Mid Jurassic. Events (5) and (6) produced cohesive breccias, which may relate to phases of Late Jurassic to Early Cretaceous rifting. The cohesive breccias are cut by event (7), another period of zeolite mineralization. One zone documents event (8), which left as a product the unconsolidated breccia. This is thought to be from activity after Late Cretaceous and possibly in the Cenozoic (Bauck, 2010).

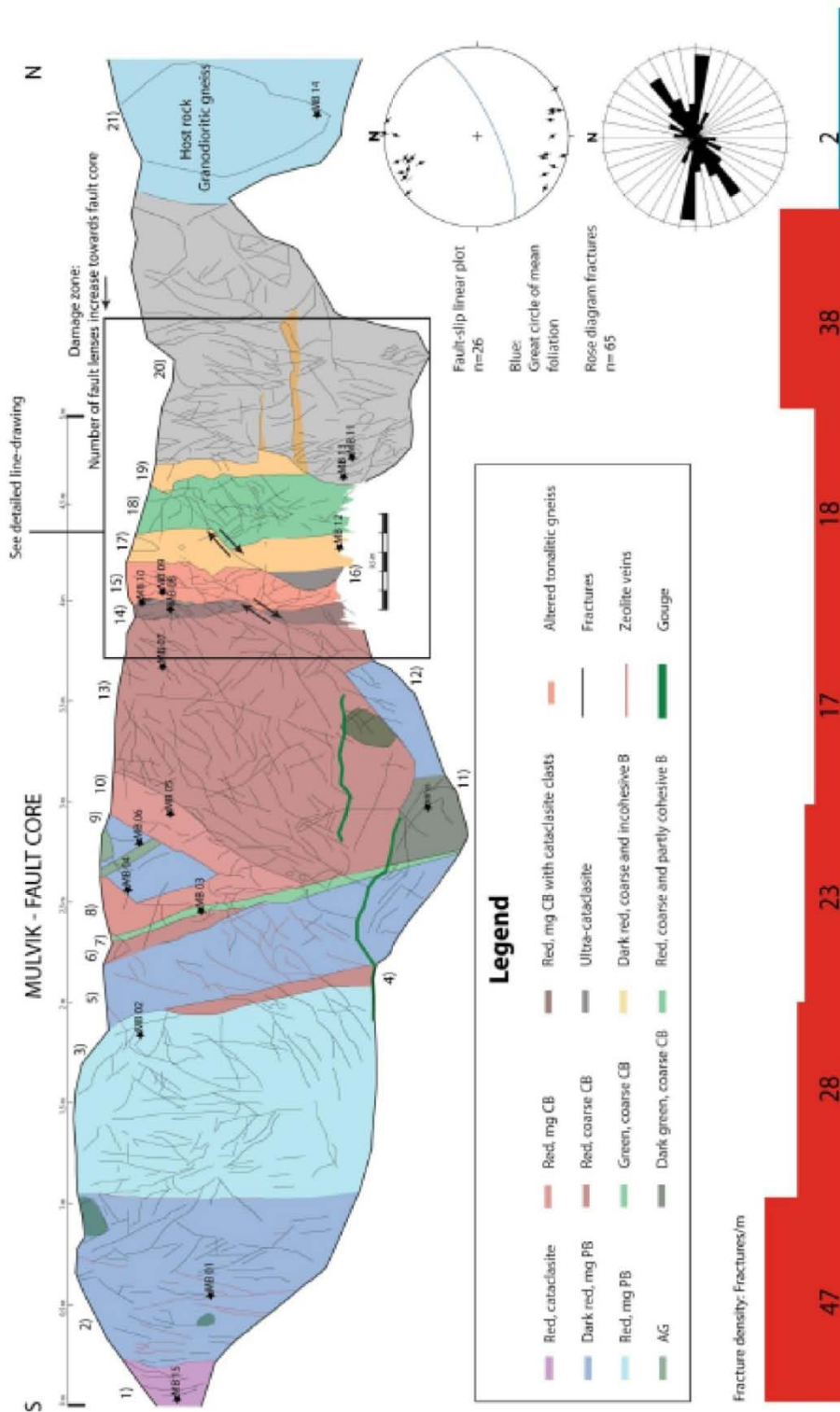


Figure 5.6.3: Fault core at main Mulvik locality. Abbreviations used are: CB – cohesive breccia, PB – proto-breccia, AG – altered gneiss, B – breccia and mg – medium-grained (1-5mm clasts). The different fault rocks are numbered from zone 1 to zone 21 from south to north. Two ‘reverse’ faults found in relation to the unconsolidated part of the Mulvik Fault core, marked with split-arrows. These are probably R-shears related to

'northern side down' faulting. They are clearly cutting zones 14), 15) and 16), but as it is going into the incohesive breccia it disappears. This is an indication of a probable establishment of these faults simultaneously with the establishment of the incohesive breccia. The histogram of the fracture density in the lower part of the figure is extracted from the fault core part (black rectangle). Fault-slip linear plot and rose diagram of measured fractures are shown down to the right in the figure. *Figure and caption from Bauck (2010).*

The majority of fault rocks described by Bauck (2010) are cohesive cataclasites and breccias. The main matrix minerals are zeolites. These are laths, probably originating from vein-growing zeolite crystals. Thus, fault movement continued after early phases of zeolite vein emplacement. Events of zeolite mineralizations seem to have occurred repeatedly, in relation to these events of brittle faulting. The last zeolite mineralization event found is of laumontite (Bauck, 2010).

6. SUMMARY AND OUTLOOK

The Mulvik Fault constituted the last stop on our tour. It also constitutes one of the last (e.g., northernmost) brittle faults of the TFZ that we have located. A small fault core is exposed near Surdadal (Axel's Fault; see Figure 3.5), but we know of no fault outcrop to its north that could be part of the TFZ. Probably not coincidentally, to the north of Axel's Fault the Scandinavian Mountains become lower, AFT juxtapositions become less resolvable, and the alpine incision class resolved by Etzelmüller et al. (2007) terminates (see Figure 3.5). There, MTFC displacement gradient is beginning to 'tip out.' As we move north, up the displacement gradient, the absolute elevation of the escarpment decreases. Alpine landforms disappear, and the degree of glacial excision becomes less and less. Hills become more rounded, with flattened tops; by the time we reach Trondheim, signs of a worn down and much older landscape abound. The landscape and AFT apparent age juxtapositions across the projected trace of the TFZ have ceased to exist (Figure 3.1).

During this field trip we witnessed the dramatic changes in Norway's topography from coast to hinterland and got an idea of the role that large-scale normal faults play in this story. Kilometer-scale uplift may have occurred along the fault system of the MTFC and may possibly continue today. One important consequence of the fault system are major rockslides that can present an acute danger to the population living in this region.

Our field trip only looked at a minute part of the stunning Norwegian coastal landscapes but we hope to have left the valid impression that similar observations can be made all along western Norway and the MTFC. Additionally, very similar patterns of reactivated Mesozoic faults, juxtaposition of differently shaped landscapes, and large-volume rockslides have been reported from Northern Norway (Osmundsen et al., 2009, 2010). The asymmetric topography and the adherence to the 'Rule of Taper' (Figure 3.7, Osmundsen and Redfield, in press) is an even more global phenomenon and should be considered when discussing mechanisms that form our worldwide passive margins. We hope that this field excursion provides a common ground with respect to Tectonic Topography on passive margins for fruitful discussions, which we hope will ensue over the next hours and days (in the bus and at the workshop, respectively).

7. CITATIONS

- Ambraseys, N., 1985. The seismicity of western Scandinavia. *Earthquake engineering and structural dynamics*, 13, 361-399.
- Anda, E., 2011. En tentativ korrelasjon mellom Moloforrasjonen og en fluvial erosjonsflate i ytre/midtre deler av Romsdal, Nordmøre og Sør Trøndelag. NGF Winter Meeting abstract.
- Bauck, M.S., 2010. Fault rock assemblages and fault architecture in the Møre-Trøndelag Fault Complex. NTNU Master's Thesis, 97 pp.
- Blundell, D.J. and Waltham, D.A., 2009. A possible glacially-forced tectonic mechanism for late Neogene surface uplift and subsidence around the North Atlantic. *Proceedings of the Geologists' Association*, 120, 98-107.
- Braathen, A., Nordgulen, Ø., Osmundsen, P.T., Andersen, T.B., Solli, A., and Roberts, D., 2000. Devonian, orogen-parallel, opposed extension of the Central Norway Caledonides. *Geology*, 28, 615-618.
- Braathen, A., Osmundsen, P.T., Nordgulen, Ø., Roberts, D. and Meyer, G., 2002. Orogen-parallel extension of the Caledonides in northern Central Norway: an overview. *Norwegian Journal of Geology*, 82, 225-241.
- Bryhni, I., Austrheim, H., Bjørnstad, Kullerud, L., and Reksten, K., 1990. Bergrunnskart Tingvoll. 1320 1 1:50000. Foreløpig utgave.
- Bungum, H., Hokland, B.K., Husebye, E.S., and Ringdal F., 1979. An exceptional intraplate earthquake sequence in Meløy, northern Norway. *Nature*, 280, 32-35.
- Chalmers, J., 2011. Flow of material under compression in the weak layers of continental crust can cause post-rift uplift of passive continental margins. *Geophysical Research Abstracts*, 13, EGU2011-5828.
- Etzelmüller, B., Romstad, B., and Fjellanger, J., 2007. Automatic regional classification of topography in Norway. *Norwegian Journal of Geology*, 87, 167-180.
- Faccenna, C., Rossetti, F., Becker, T.W., Danesi, S., and Morelli, A., 2008. Recent extension driven by mantle upwelling beneath the Admiralty Mountains (East Antarctica). *Tectonics*, 27, TC4015, doi:10.1029/2007TC002197.
- Faleide, J.I., Tsikalas, F., Breivik, A.J., Mjelde, R., Ritzmann, O., Engen, Ø., Wilson, J., and Eldholm, O., 2008. Structure and evolution of the continental margin off Norway and the Barents Sea. *Episodes*, 31, 82-91.
- Furseth, Å., 2006. Skredulykker I Norge. ISBN 8252930433 207 pp.
- Gabrielsen, R.H. and Ramberg, B., 1979. Fracture patterns in Norway from LandSAT imagery: results and potential use. *Proceed. Norwegian Sea Symp., Tromsø*, Norwegian Petroleum Society, NSS/23, 1-28.
- Gawthorpe, R.L. and Leeder, M.R., 2000. Tectono-sedimentary evolution of active extensional basins. *Basin Research*, 12, 195-218.
- Grunnalleite, I. and Gabrielsen, R.H., 1995. The structure of the Møre Basin. *Tectonophysics*, 252, 221-251.
- Grønlie, A. and Roberts, D., 1989. Resurgent strike-slip duplex development along the Hitra-Snåsa and Verran faults, Møre-Trøndelag Fault Zone, Central Norway. *Journal of Structural Geology*, 11, 295-305.

- Grønlie, A. and Torsvik, T., 1989. On the origin and age of hydrothermal thorium enriched carbonate veins and breccias in the Møre-Trøndelag Fault Zone, central Norway. *Norwegian Journal of Geology*, 69, 1-19.
- Grønlie, A., Nilsen, B., and Roberts, D., 1991. Brittle deformation history of fault rocks on the Fosen Peninsula, Trøndelag, central Norway. *Nor. Geol. Unders. Bull.*, 421, 39-57.
- Grønlie, A., Naeser, C.W., Naeser, N.D., Mitchell, J.G., Sturt, B.A., and Ineson, P., 1994. Fission track and K/Ar dating of tectonic activity in a transect across the Møre-Trøndelag Fault Zone, Central Norway. *Norwegian Journal of Geology*, 74, 24-34.
- Hendriks, B.W.H., Andriessen, P., Huigen, Y., Leighton, C., Redfield, T., Murrell, G., Gallagher, K., and Nielsen, S. B., 2007. A fission track data compilation for Fennoscandia. *Norwegian Journal of Geology*, 87, 143-155.
- Hendriks, B.W.H., Osmundsen, P.T. and Redfield, T.F., 2010. Normal faulting and block tilting in Lofoten and Vesterålen constrained by Apatite Fission Track data. *Tectonophysics*, 485, 154-163.
- Hicks, E., Bungum, H., and Lindholm, C., 2000. Stress inversions of earthquake focal mechanism solutions from onshore and offshore Norway. *Nor. Geol. Tidsskr.*, 80, 235-250.
- Hola, O., 1976. Folkeliv og tradisjon frå Nesset, bnd 1, Molde 2000 - Austigard, Bjørn: Nytt om Tjellefonna. *Romsdalsmuseets årbok 1976*, Idnr. 15331.
- Holtedahl, H., 1953. On the oblique uplift of some northern lands. *Norsk Geogr. Tidsskr.*, 14, 132-139.
- Høst, J., 2006: Store fjellskred i Norge. Utarbeidet av NGU, Direktoratet for samfunnssikkerhet og beredskap, Statens landbruksforvaltning, Statens vegvesen, Jernbaneverket og Statens kartverk. Utredning for Landbruks- og matdepartementet på vegne av 6 departementer. 82 pp.
- Krabbendam, M. and Dewey, J.F., 1998. Exhumation of UHP rocks by transtension in the Western Gneiss Region, Scandinavian Caledonides. *In: R.E. Holdsworth, R.A. Strachan, and J.F. Dewey, (eds.), Continental transpressional and transtensional tectonics*. Geol. Soc. London Special Publication, 135, 159-181.
- Leeder, M.R. and Gawthorpe, R.L., 1987. Sedimentary models for extensional tiltblock/ half-graben basins. *In: M.P. Coward, J.F. Dewey, and P.L. Hancock (eds.), Continental Extensional Tectonics*. Geol. Soc. London Special Publications, 28, 139-152.
- Leeder, M.A. and Jackson, J.A., 1993. The interaction between normal faulting and drainage in active extensional basins, with examples from the western United States and central Greece. *Basin Research*, 5, 79-102.
- Lidmar-Bergström, K., Ollier, C.D., and Sulebak, J.R., 2000. Landforms and uplift history of Southern Norway. *In: J. Chalmers and S. Cloetingh (eds.), Neogene uplift and tectonics around the North Atlantic*. *Global and Planetary Change*, 24, 211-231.
- Lidmar-Bergström, K., Näslund, J.-O., Ebert, K., Neubeck, T., and Bonow, J.M., 2007. Cenozoic landscape development in northern Scandinavia. *Norwegian Journal of Geology*, 87, 181-196.
- Lundin, E.R. and Doré, A.G., 2011. Hyperextension, serpentinization, and weakening: A new paradigm for rifted margin compressional deformation. *Geology*, 39, 347-350, doi:10.1130/G31499.1.

- Løseth, H., 2005. The rise of the Norwegian mountains – seen in a shelf perspective. NGF Abstr., Proceed. Norw. Geol. Soc., 1, 70.
- Løseth, H. and Tveten, E., 1996. Post-Caledonian structural evolution of the Lofoten and Vesterålen offshore and onshore areas. Norwegian Journal of Geology, 76, 215-230.
- Manatschal, G., Froitzheim, N., Rubenach, M., and Turrin, B.D., 2001. The role of detachment faulting in the formation of an ocean-continent transition: insights from the Iberia Abyssal Plain. In: R.C.L. Wilson, R.B. Whitmarsh, B. Taylor, and N. Froitzheim (eds.), *Non-volcanic rifting of continental margins: a comparison of evidence from land and sea*. Geol. Soc. London Special Publications, 187, 1-24.
- Masson, D.G., Cartwright, J.A., Pinheiro, L.M., Whitmarsh, R.B., Beslier, M.-O., and Roeser, H., 1994. Compressional deformation at the continent-ocean transition in the NE Atlantic. J. Geol. Soc. London, 15, 607-613.
- McKenzie, D., 1978. Some remarks on the development of sedimentary basins. EPSL, 40, 25-32.
- Morsing, C., 1757. En kortileg beskrivelse over Jordskiælvvet, og Fieldets Nedfald, Som skede udj Nettet-Præstegjæld i Romsdahls Provstie, og Throntheims Stift udj Norge, nestafvigte Aar, Natten til dend 23 Februarij 1756. Kiøbenhafn, 13 December, 1757. Norsk Historisk Kjeldskrift Institutt, Boks 23, Kringsjå, Oslo 8, Norge.
- Mosar, J., Lewis, G., and Torsvik, T.H., 2002. North Atlantic sea-floor spreading rates: implications for the Tertiary development of inversion structures of the Norwegian–Greenland Sea. J. Geol. Soc. Lond., 159, 503-515.
- Munch, P.A., 1850. Übersicht der Orographie Norwegens. In: B.M. Keilhau (ed.) *Gaca Norvegica*, 503-516. Christiana.
- Nasuti, A., Chawshin, K., Dalsegg, E., Tønnesen, J.F., Ebbing, J., and Gellein, J., 2009. Electrical resistivity and refraction seismics over a segment of the Møre-Trøndelag Fault Complex. NGU report 2009.037, 37 pp.
- Nasuti, A., Beiki, M., and Ebbing, J., 2010. Gravity and magnetic data acquisition over a segment of the Møre-Trøndelag Fault Complex. NGU report 2010.049, 42 pp.
- Nasuti, A., Pascal, C., Ebbing, J., and Tønnesen, J.F., 2011. Geophysical characterisation of two segments of the Møre-Trøndelag Fault Complex, Mid-Norway. Solid Earth Discuss., 3, 159-186.
- Nielsen S.B., Gallagher K., Leightonc, C., Balling, N., Svenningsen, L., Jacobsen B.H., Thomsen, E., Nielsen, O.B., Heilmann-Clausen, C., Egholm, D.L., Summerfield, M.A., Clausen, O.R., Piotrowski, J.A., Thorsen, M.R., Huuse, M., Abrahamsen, N., King, C., and Lykke-Andersen, H., 2009. The evolution of western Scandinavian topography: A review of Neogene uplift versus the ICE (isostasy–climate–erosion) hypothesis. Journal of Geodynamics, 47, 72-95.
- Olesen, O., Skelton, A., Ebbing, J., and Gernigon, L., 2006. Is the Neogene uplift of the circum Atlantic margin caused by serpentinisation of the lithospheric mantle? Geophysical Research Abstracts, 8, 09992.
- Osmundsen, P.T. and Ebbing, J., 2008. Styles of extension offshore Mid Norway and implications for mechanisms of crustal thinning at passive margins. Tectonics, 27, TC6016, doi:10.1029/2007TC002242.
- Osmundsen, P.T. and Redfield, T.F., in press. Crustal taper and topography at passive continental margins. Terra Nova.

- Osmundsen, P.T., Eide, E.A., Haabesland, N.E., Roberts, D., Andersen, T.B., Kendrick, M., Bingen, B., Braathen, A., and Redfield, T.F. 2006. Kinematics of the Hoybakken detachment zone and the More-Trondelag Fault Complex, central Norway. *JGSL*, 163, 303-318.
- Osmundsen, P.T., Henderson, I., Lauknes, T.R., Larsen, Y., Redfield, T.F. and Dehls, J., 2009. Tectonic controls on topography and mass-wasting processes in Northern Norway. *Geology*, 37, 135-138.
- Osmundsen, P.T., Redfield, T.F., Anda, E., Hendriks, B., Henderson, I., Dehls, J., Lauknes, T.R., Fredin, O. and Davidsen, B. 2010. The tectonic significance of Alpine landscapes in Norway. *J. Geol. Soc. London*, 167, 83-98. doi:10.1144/0016-76492009-019.
- Péron-Pinvidic, G., Manatschal, G., Dean, S. and Minshull, T., 2008. Compressional structures on the West Iberia rifted margin: what controls their distribution? *In: H., Johnson et al. (eds.), The Nature and Origin of Compression in Passive Margins*. Geol. Soc. London Special Publications, 306, 169-183. doi:10.1144/SP306.8.
- Péron-Pinvidic, G. and Manatschal, G., 2009. The final rifting evolution at deep magma-poor passive margins from Iberia-Newfoundland: a new point of view. *Int. J. Earth Sci. (Geol. Rundsch.)*, doi:10.1007/s00531-008-0337-9.
- Phillips, I.F. and Schumm, S.A., 1987. Effect of regional slope on drainage networks. *Geology*, 15, 813-816.
- Ramberg, I.B., Gabrielsen, R.H., Larsen, B.T., and Solli, A., 1977. Analysis of fracture pattern in Southern Norway. *Geologie en Mijnbouw*, 56, 295-310.
- Redfield, T.F., 2010. On apatite fission track dating and the Tertiary evolution of West Greenland topography. *J. Geol. Soc. London*, 167, 261-271. doi:10.1144/0016-76492009-036.
- Redfield, T.F. and Osmundsen, P.T., 2009. The Tjellefonna fault system of Western Norway: Linking late-Caledonian extension, post-Caledonian normal faulting, and Tertiary rock column uplift with the landslide-generated tsunami event of 1756. *Tectonophysics*, 474, 106-123.
- Redfield, T.F. and Osmundsen, P.T., 2011. Mesozoic crustal architecture defines Scandinavia's present-day Geomorphology. *Geophysical Research Abstracts*, 13, EGU2011-3312.
- Redfield, T.F., Torsvik, T.H., Andriessen, P.A.M., and Gabrielsen, R.H., 2004. Mesozoic and Cenozoic tectonics of the Møre-Trøndelag Fault Complex, central Norway: constraints from new apatite fission track data. *Physics and Chemistry of the Earth*, 10, 29, 673-682.
- Redfield, T.F., Braathen, A., Gabrielsen, R.H., Osmundsen, P.T., Torsvik, T., and Andriessen, P.A.M., 2005a. Late Mesozoic to Early Cenozoic components of vertical separation across the Møre-Trøndelag Fault Complex, Norway. *Tectonophysics*, 395, 233-249.
- Redfield, T.F., Osmundsen, P.T. and Hendriks, B.W.H., 2005b. The role of fault reactivation and growth in the uplift of western Fennoscandia. *J. Geol. Soc. London*, 162, 1013-1030.
- Rindstad, B.I., and Grønlie, A., 1986. LandsAT TM data used in the mapping of large scale geological structures in coastal areas of Trøndelag, Central Norway. *In: Proceedings of a Workshop on LandsAT Thematic Mapper applications*, 169-181. Frascati, Italy.
- Rohrman, M., van der Beek, P., Andriessen, P.A.M., and Cloetingh, S., 1995. Meso-Cenozoic morphotectonic evolution of southern Norway: Neogene domal uplift inferred from apatite fission track thermochronology. *Tectonics*, 14, 704-718.

- Séranne, M., 1992. Late Paleozoic kinematics of the Møre-Trøndelag Fault Zone and adjacent areas, central Norway. *Norwegian Journal of Geology*, 72, 141-158.
- Sibson, R.H., 1977. Fault rocks and fault mechanisms. *Journal of the Geological Society*, 133, 191-213.
- Skelton, A. and Jakobsson, M., 2007. Could peridotite hydration reactions have provided a contributory driving force for Cenozoic uplift and accelerated subsidence along the margins of the North Atlantic and Labrador Sea? *Norwegian Journal of Geology*, 87, 21-28.
- Sommaruga, A. and Bøe, R., 2002. Geometry and subcrop maps of shallow Jurassic basins along the Mid-Norway coast. *Marine Petroleum Geology*, 19, 1029–1042.
- Stiberg, J.P., 1993. Apatite fission track analysis from the Western Gneiss Region, preliminary results: constraints to the Cenozoic uplift of the Norwegian passive margin (abstract). *Geonytt*, 1, 46.
- Stüwe, K., 1991. Flexural constraints on the denudation of asymmetric mountain belts. *J. Geophys. Res.*, 96, 10401-10408.
- Torske, T., 1972. Tertiary oblique uplift of Western Fennoscandia; Crustal warping in connection with rifting and break-up of the Laurasian continent. *Nor. Geol. Unders. Bull.*, 273, 43-48.
- Torsvik, T.H., Sturt, B.A., Ramsay, D.M., Grønlie, A., Roberts, D., Smethurst, M., Atakan, K., Bøe, R., and Walderhaug, H.J., 1989. Palaeomagnetic constraints on the early history of the Møre-Trøndelag Fault Zone, central Norway. *In: C. Kissel and C. Lai (eds.), Paleomagnetic Rotations and Continental Deformation*, 431-457, Kluwer Academic Publishers.
- Trygstad, S., 2002. Sprengning av tomt, Fjelltunveien 31, Ålesund. Rapport nr. 1022-1. GeoBergen, Øvre Sædalsvei 20, Bergen, Norway. 9 pp.
- Tvedt, E., Havskov, J., Atakan, K., Storheim, B., and Kjaergaard, A.L., 2002. Seismicity of Norway, 1990-2000. Institute of Solid Earth Physics, University of Bergen, Bergen.
- Watts, L. M., 2001. The Walls Boundary fault zone and the Møre-Trøndelag Fault Complex: a case study of two reactivated fault zones, Ph.D. Thesis, University of Durham.
- Weissel, J. K. and Karner, G.D., 1989. Flexural uplift of rift flanks due to mechanical unloading of the lithosphere during extension, *J. Geophys. Res.*, 94, 13919-13950.